THE JOURNAL OF BIOLOGICAL CHEMISTRY VOL. 287, NO. 50, pp. 41757–41773, December 7, 2012

LETM Proteins Play a Role in the Accumulation of Mitochondrially Encoded Proteins in *Arabidopsis thaliana* and *AtLETM2* Displays Parent of Origin Effects*[S]

Received for publication, May 22, 2012, and in revised form, October 1, 2012 Published, JBC Papers in Press, October 5, 2012, DOI 10.1074/jbc.M112.383836

Botao Zhang[‡], Chris Carrie[‡], Aneta Ivanova[‡], Reena Narsai[‡§], Monika W. Murcha[‡], Owen Duncan[‡], Yan Wang[‡], Simon R. Law[‡], Verónica Albrecht[¶], Barry Pogson[¶], Estelle Giraud[‡], Olivier Van Aken[‡1], and James Whelan[‡2]

From the [‡]Australian Research Council Centre of Excellence in Plant Energy Biology and [§]Centre for Computational Systems Biology, Bayliss Building M316 University of Western Australia, 35 Stirling Highway, Crawley 6009, Western Australia, Australia and the [¶]Australian Research Council Centre of Excellence in Plant Energy Biology, Research School of Biology, Australian National University, Acton 2601, Australian Capital Territory, Australia

Background: Plants contain homologs of the conserved mitochondrial protein LETM1.
Results: AtLETM1 and AtLETM2 are important proteins for accumulation of ATP synthase proteins in *Arabidopsis thaliana*, and double mutants are not viable. *AtLETM2* expression displays parent of origin effects during seed development.
Conclusion: Accumulation of mitochondrially encoded proteins is under maternal control during early development.
Significance: This work reveals that mitochondrial gene expression is under maternal control early in development.

The *Arabidopsis thaliana* genome contains two genes with homology to the mitochondrial protein LETM1 (leucine zipper-EF-hand-containing transmembrane protein). Inactivation of both genes, *Atletm1* and *Atletm2*, together is lethal. Plants that are hemizygous for *AtLETM2* and homozygous for *Atletm1* (*letm1*(−/−) *LETM2*(+/−)) displayed a mild retarded growth phenotype during early seedling growth. It was shown that accumulation of mitochondrial proteins was reduced in hemizygous (*letm1*(−/−) *LETM2*(+/−)) plants. Examination of respiratory chain proteins by Western blotting, blue native PAGE, and enzymatic activity assays revealed that the steady state level of ATP synthase was reduced in abundance, whereas the steady state levels of other respiratory chain proteins remained unchanged. The absence of a functional maternal *AtLETM2* allele in an *Atletm1* mutant background resulted in early seed abortion. Reciprocal crosses revealed that maternally, but not paternally, derived *AtLETM2* was absolutely required for seed development. This requirement for a functional maternal allele of *AtLETM2* was confirmed using direct sequencing of reciprocal crosses of Col-0 and L*er* accessions. Furthermore, *AtLETM2* promoter β-glucuronidase constructs displayed exclusive maternal expression patterns.

The endosymbiotic event that led to the formation of mitochondria occurred over one billion years ago (1), yet the mitochondrial genome from a wide variety of phylogenetic lineages still contains a small number of genes that encode from three to over 50 proteins (2–5). These proteins are each found in multisubunit protein complexes and must be assembled along with nucleus-encoded proteins to form functional protein complexes (6). Although the coding capacity of mitochondria is ≤5% of the total number of proteins that are located in mitochondria, which is estimated to be >1000 (7), the proteins encoded in the mitochondrial genome are essential for normal growth and development. In many cases, mutations or disruption of mitochondrial genes results in a lethal or severely retarded growth phenotype (8). The majority of the proteins required for the transcription, translation, and replication of mitochondrial DNA are encoded in the nucleus and must be translated in the cytosol before being imported into the mitochondrion (7). Literally hundreds of nucleus-located genes are required for the expression of mitochondrial genes, from the proteins required for DNA replication and transcription to processing of transcripts. Translation requires discrete translation machinery, ranging from ribosomes to aminoacyl-tRNA synthetases and various other factors that make up the translational machinery. In higher plants, hundreds of genes that encode pentatricopeptide proteins are required for editing and processing of mitochondrial RNA (9), and many aspects of organelle transcription and RNA processing have been studied in detail. In contrast, little is known about factors that may affect or regulate the translation of organelle-encoded transcripts in plant mitochondria (10).

Yeast are distinct from other eukaryotes in that mitochondrial inheritance is biparental. In multicellular eukaryotes, inheritance of mitochondria is uniparental (11), with some minor exceptions, such as the parental "leakage" observed in *Silene vulgaris* (12). The precise mechanism(s) defining maternal inheritance of mitochondria are not clear, but the identification and characterization of specific endonucleases expressed in pollen cells in *Arabidopsis thaliana* (*Arabidopsis*) provides a mechanism that selectively degrades paternal mitochondrial DNA (13). Although the nuclear genome is clearly inherited in a Mendelian manner, studies have shown that sub-

* This work was supported by a Chinese Scholarship Council Scholarship (to B. Z.) and the Australian Research Council Centre of Excellence Program CEO561495.
[S] This article contains supplemental Tables 1–4 and Figs. 1–4.
[1] Supported by Australian Research Council APD Discovery Fellowship DP110102868.
[2] To whom correspondence should be addressed. Tel.: 61-8-6488-1749; Fax: 61-8-6488-4401; E-mail: jim.whelan@uwa.edu.au.

sets of genes are preferentially expressed based on the parent of origin and are defined as imprinted genes (14). Imprinting primarily occurs in the endosperm in *Arabidopsis* and is proposed to occur because of the parental conflict hypothesis (15). This hypothesis states that in mammals and flowering plants with multiple embryos, where different parental fertilization of embryos can occur and where the embryo receives nutrition from the maternal tissue via the placenta or endosperm, there is a conflict because the male parent would favor investment of more resources in the embryo fertilized by its gametes, whereas the female would favor equal investments in all embryos. This hypothesis is proposed as a driving force for exclusive or biased maternal expression of genes during embryo development.

Here, we detail the characterization of two nucleus-encoded, mitochondrial proteins, AtLETM1 and AtLETM2 (leucine zipper-EF-hand-containing transmembrane protein). AtLETM1 and AtLETM2 show similarity to the mammalian protein LETM1 and yeast Mdm38 (16, 17). Human LETM1 is associated with Wolf-Hirschhorn syndrome. Yeast *mdm38* mutants display abnormal mitochondrial morphology and potassium homeostasis (18, 19). The demonstration that LETM1 in mitochondria from *Drosophila* mediates Ca^{2+}/H^{+} supports a role in maintaining ionic balance (20). In addition, a role for Mdm38 in mitochondrial translation has been shown in yeast. In yeast, at least three proteins bind to ribosomes to affect translation: Oxa1, Mba1, and Mdm38 (16). Specifically, Mdm38 functions as a membrane-bound ribosome receptor that has overlapping functions with Mba1 and is required for the translation of *COX1* and *CYTB* mRNA in yeast; a double mutant of *mdm38* and *mba1* lacks complex III and IV (16). This role in translation is distinct from that in regulating ionic balance because the latter can be rescued by nigericin, whereas the former cannot (16). Additionally, it should be noted that a variety of translational activators have been identified in yeast that are specific for each transcript (21), and substituting the *COXI* UTRs for that of *COX2* results in the recovery of translation of *COX1* (16). We show that AtLETM1 and AtLETM2 are required for efficient translation in mitochondria in *Arabidopsis*. We demonstrate that maternal expression of *LETM2* is required for successful seed development and, furthermore, that the amount of LETM2 protein in mitochondria is correlated with gene dosage for *LETM2*.

EXPERIMENTAL PROCEDURES

T-DNA Insertion Lines—The following T-DNA insertion lines were obtained from the ABRC stock center: *AtLETM1* (At3g59820): SALK_067558C (*letm1-1*), SALK_058471 (*letm1-2*) and *AtLETM2* (At1g65540): SALK_068877 (*letm2-1*), WISCDSLOXHS169_10B (*letm2-2*). Plants were genotyped by PCR, and the insert positions were confirmed by sequencing with T-DNA left border primers. Primer sequences are listed in supplemental Table 1. Phenotype analysis of all mutants was carried out as described by Boyes *et al.* (22).

Construction of GFP Fusion Vectors—Coding sequences for *LETM1* and *LETM2* were amplified from *Arabidopsis* cDNA using standard protocols with the Roche Expand High Fidelity PCR system (Roche Applied Science), using gene-specific primers flanked by Gateway recombination cassettes (Invitrogen) (supplemental Table 1). The first 300 bp as well as the full-length coding sequences were cloned into pDONR201 according to the manufacturer's instructions. Cloning into the final GFP vectors was as described by Carrie *et al.* (23). As a mitochondrial marker, the alternative oxidase (AOX)[3] targeting signal of 42 amino acids fused to RFP was used (23).

Stable Transformation, Biolistic Transformation, and Microscopy—To monitor mitochondrial morphology in the hemizygous AtLETM2 (*letm1*(−/−) *LETM2*(+/−)), a cross was carried out between the aforementioned hemizygous mutant and a line of *Arabidopsis* stably transformed with a mitochondrial targeted GFP and backcrossed to obtain the *letm1*(−/−) *LETM2*(+/−) hemizygous genotype. The resulting seeds were then grown on Murashige and Skoog (MS) medium. Biolistic co-transformation of the GFP and RFP fusion vectors was performed on *Arabidopsis* cell culture and onion epidermal cells as previously reported (23). In brief, GFP and RFP plasmids (5 μg each) were co-precipitated onto gold particles and transformed using a PDS-1000/He biolistic transformation system (Bio-Rad). Two ml of *Arabidopsis* cell suspension (on a paper filter) or freshly peeled onion epidermal cells were placed on osmoticum medium and bombarded. Cells were then incubated for 24–48 h at 22 °C in the dark. GFP and RFP expression in both the permanent and transient transformants were visualized using a BX61 Olympus microscope (Olympus, Melbourne, Australia) using excitation wavelengths of 460/480 nm (GFP) and 535/555 nm (RFP) and emission wavelengths of 495–540 nm (GFP) and 570–625 nm (RFP). Subsequent images were captured using Cell® imaging software as described previously (24).

Mitochondrial Purification—To obtain mitochondria for biochemical analysis, wild-type (Col-0) and hemizygous AtLETM2 (*letm1*(−/−) *LETM2*(+/−)) seeds were first vertically grown on MS agar plates for 3 days under continuous light conditions before being transferred to liquid culture medium to allow visual selection of hemizygous AtLETM2 seedlings. Seedlings were grown for another 7 days in MS medium under long day conditions (16 h light, 8 h darkness) before harvesting for mitochondrial preparations. Mitochondria were harvested from 10-day-old seedlings as described previously (25). Typically 2–3 mg of mitochondrial protein were obtained from ~20 g of starting tissue. Mitochondrial protein concentrations were determined using the Coomassie protein assay reagent (Thermo Scientific, Rockford, IL) in triplicate.

In Organello Protein Synthesis—*In organello* protein synthesis assays were carried out as described previously (10), using freshly prepared mitochondria. The reactions were resolved by SDS-PAGE (26), and the incorporation of [^{35}S]Met into protein bands was determined by exposing a phosphorimaging plate to a dried gel for 48 h. The exposed plate was visualized using the Personal Molecular Imager (Bio-Rad) at high resolution. Radiolabeled bands corresponding to the correct apparent molecular weights for ATPα, CYTB, COXII, NAD9, NAD6, and ATP9 where quantitated at 10, 30, and 60 min time points using

[3] The abbreviations used are: AOX, alternative oxidase; MS, Murashige and Skoog; GUS, β-glucuronidase; BN-PAGE, blue native PAGE; PiC, mitochondrial phosphate carrier; L*er*, Landsberg *erecta*.

Quantity One software (Bio-Rad). Radiolabeled bands where uniformly boxed, and the pixel density was determined for each band minus the background. The pixel densities were expressed relative to Col-0 at 60 min, which was adjusted to 1. Three biological replicates were performed and quantitated, and the average and S.E. relative to Col-0 were determined. The incorporation of [^{35}S]Met was compared for each band across the four genotypes to give the relative efficiency of translation of each protein in each genotype (Fig. 4*A*), and also the incorporation of [^{35}S]Met into each band was expressed as a percentage of the total incorporation for the six identified bands in each genotype, to give a measure of the total incorporation into each band in each genotype (supplemental Fig. 4).

In Vitro Import Studies—[^{35}S]Met-labeled precursor proteins for AOX (X68702) (27) and mitochondrial phosphate carrier (PiC) (AB016064) (28, 29) were synthesized using rabbit reticulocyte TNT *in vitro* transcription/translation lysate (Promega, Melbourne, Australia) as described previously (27). Time course analysis of precursor protein import into intact mitochondria isolated from wild-type (Col-0) or mutant plants was performed as described previously, and radiolabeled imported proteins were quantified at each time point and normalized to the highest time point for Col-0, which was set to 100% using Quantity One software (Bio-Rad). Three biological replicates were carried out for each mutant and precursor protein, and the average and S.E. of import amount relative to Col-0 were determined (25).

Immunodetection of Proteins—Isolated mitochondria (15 μg) were resolved by SDS-PAGE, transferred to Hybond-C extra nitrocellulose membrane, and immunodetected as outlined previously (23). To generate antibodies to AtLETM1, recombinant proteins containing amino acids 387–525 (LETM1 AB1) and amino acids 540–667 (LETM1 AB2) of AtLETM1 fused to an N-terminal His_6 affinity purification tag were expressed in *Escherichia coli* strain BL21 (DE3) pLys (Stratagene, La Jolla, CA) using the pDEST17 expression vector (Invitrogen). The recombinant protein was purified by denaturing immobilized metal affinity chromatography, using the Profinia protein purification system (Bio-Rad). The resultant eluate was separated by SDS-PAGE, and the recombinant protein was extracted using a Bio-Rad model 422 Electro-Eluter. Buffer exchange was performed using an Amicon Ultracel 5K centrifugal filter device (Millipore) such that the antigen was resuspended in PBS solution, recovering a total of 3 mg (LETM1 AB1) and 4 mg (LETM1 AB2) of proteins for inoculation. Four separate doses were administered to a rabbit at regular intervals over a 3-month period using standard protocols and Freund's complete adjuvant solution (30). Other antibodies used have been described previously: RISP (31), NAD9 (32), uncoupling protein (33), TOM40 (24), and TIM17-2 (34). ATPβ and COXII were obtained from Agrisera (Vannas, Sweden). ATPα, porin, E1α, and AOX were obtained from Dr. Tom Elthon (University of Nebraska, Lincoln, NE). Detection of cross-reacting products was carried out using chemiluminescence, and the signal was captured using ImageQuant RT ECL (GE Healthcare) with the signal intensity (pixel intensity) adjusted relative to wild type (Col-0) and set to 100. The abundance of each protein was normalized to wild type (Col-0), which was set to 100%. Three biological replicates were carried out, and the average and S.E. relative to wild type (Col-0) were determined.

Promoter Reporter Analysis—1 kb region upstream of the start codons of LETM1 and LETM2 was cloned into pBGWFS7 (35) in fusion with GUS, by Gateway recombination (Invitrogen). The homozygous promoter-GUS fusion transgenic plants from five independent lines were stained with 5-bromo-4-chloro-3-indolyl-β-glucuronic acid (GoldBio) as described (36).

Analysis of Gametophytes and Seed Development and Sequencing of LETM2 Transcript from Embryo and Endosperm—Unfertilized ovules and seeds at different developmental stages of Col-0 and AtLETM mutant lines were cleared using chloral hydrate and mounted on microscope carriers. Microscopy was then performed on a Zeiss Axioplan differential interference contrast microscope. Endosperm nuclei were counted using images displayed on a video monitor attached to the microscope, as reported before (37). Viability staining and counting of pollen were performed as described previously (38). Statistical tests for viable/aborted ratios and progeny genotyping of the reciprocal crosses were performed using a Pearson's χ^2 test. Flower buds of Col-0 and Landsberg *erecta* (L*er*) plants were emasculated and reciprocally pollinated 36 h later. Embryo and endosperm were dissected under a dissecting microscope 6 days after pollination, which corresponded to the late torpedo stages of embryogenesis. Embryos were washed to remove contaminating endosperm and seed coats using RLT buffer (RNAeasy kit, Qiagen, Melbourne, Australia). Approximately 10 siliques were dissected, and total RNA was extracted using the RNAeasy kit plus DNase digestion. Three independent sets of total RNA were obtained from each direction of the crosses. Total RNA was converted to double-stranded cDNA using the Invitrogen cDNA synthesis kit (Melbourne, Australia). Fragments of the *LETM2* gene, containing SNP between Col-0 and L*er* ecotypes, were amplified with primers 5′ -GTTGACG-GCAGCATGTTTGGG-3′ and 5′-CTGGAAAGATGAATT-TAAGTC-3′ and sequenced by the Sanger method.

Quantitative RT-PCR—RNA isolation, cDNA generation, and quantitative RT-PCR on the mitochondrial transcriptome were performed as described (39) using the LightCycler 480 SYBR Green I Master Mix (Roche Applied Science) and the primer pairs listed in supplemental Table 1 on a LightCycler 480 real-time PCR system (Roche Applied Science). The nuclear *18S* rRNA gene was used for data normalization. Transcripts were measured in technical triplicate from three independent RNA isolations in separate experiments.

Global Transcript Analysis—Analysis of the changes in transcript abundance between Col-0, and double mutants was performed using Affymetrix GeneChip™ *Arabidopsis* ATH1 Genome Arrays (Affymetrix, Santa Clara, CA), along with preliminary data quality assessment, as described previously (31). Once processed, GC Robust Multiarray Average normalized gene expression values were analyzed to identify differentially expressed genes by a regularized *t* test based on a Bayesian statistical framework using the software program Cyber-T (40) as in Ref. 39. Changes were considered significant at an false discovery rate correction level of PPDE ($>P$) $>$0.95 and a -fold change greater than 1.5. Hierarchical clusters were generated in

Partek Genomics Suite software, version 6.3 (Partek, St. Louis, MO) using Euclidean distance and average linkage measures. Overrepresented gene ontology full categories were identified using a hypergeometric test with a significance threshold of 0.05 after a Benjamini and Hochberg false discovery rate correction (41).

Measurement of ATP Concentration—Total ATP levels were measured using the ATP bioluminescent assay kit (Sigma). Leaves from Col-0 and hemizygous AtLETM2 plants were frozen in liquid nitrogen and ground using a ball mixer. Plant extracts were resuspended in 500 μl of 2.3% (v/v) TCA. After centrifugation for 15 min at 20,000 $\times$ *g*, the supernatant was recovered and neutralized using a few drops of 2.5 M K_2CO_3. Total ATP levels were measured using the ATP bioluminescent assay kit (Sigma).

Mitochondrial Respiration and Complex Activity Assays—Isolated mitochondria of *in vitro* grown seedlings were used for respiration measurements and succinate dehydrogenase activity assays as described previously (42).

Starch Staining—For the staining of plants for starch, leaves were boiled in 80% (v/v) ethanol in order to remove chlorophyll. After washing three times in water, leaves were placed in 50% (v/v) Lugol solution (Sigma) for 5 min. Leaves were destained in water for 60 min before being imaged.

Identification of Protein Complex Subunits—Isolated mitochondria were separated by blue native PAGE as described previously (43). Complexes of interest were excised and were destained in 50% (v/v) acetonitrile, 10 mM NH_3HCO_3 before incubation in 1% (w/v) SDS, 1% (v/v) β-mercaptoethanol at 60 °C for 30 min. Gel fragments were dried at 60 °C for 20 min before digestion and analysis by LC-MS as described previously (44).

Accession Numbers—The genes described in this article correspond to the following Arabidopsis Genome Initiative codes: At3g59820 (AtLETM1) and At1g65540 (AtLETM2). A complete list of oligonucleotides used in this study is available in supplemental Table 1. All raw and processed microarray data files can be found at ArrayExpress under the accession number E-MEXP-3328 (www.ebi.ac.uk).

RESULTS

AtLETM1 and AtLETM2 Are Conserved Mitochondrial Proteins—Previous studies have defined a number of nucleus-located genes encoding mitochondrial proteins that respond to a wide variety of stresses in *Arabidopsis* (45). Several of these genes have no defined function, and many have additional alleles that display high levels of sequence identity and constitutive expression, suggesting basic housekeeping functions. Thus, we undertook studies to determine the function of these genes. One gene, encoded at locus At3g59820, was annotated as a putative calcium-binding protein, but no other functional data have been reported. A close homolog of this gene, At1g65540, was identified in the *Arabidopsis* genome, with the predicted protein displaying 58% amino acid identity and 72% amino acid similarity. A BLAST search identified these genes as homologous to the mitochondrial proteins, LETM1, in humans (46) and Mdm38 in yeast (47). These two orthologs display 48 and 43% amino acid identity, respectively, in the conserved LETM1 domain of AtLETM1. Therefore, the *Arabidopsis* genes were labeled *AtLETM1* (At3g59820) and *AtLETM2* (At1g65540). Structural analysis revealed that all LETM1-like proteins contain a central conserved domain, termed the LETM1-like domain, which features a highly conserved 22-amino acid transmembrane domain (Fig. 1*A*). Furthermore, the plant and animal lineages have acquired a C-terminal Ca^{2+}-binding EF-hand domain, which is absent from the yeast lineage. The leucine zipper domain seems to be only present in the animal LETM1-like proteins and has diverged in plants and yeast.

Simultaneous Mutations in AtLETM1 and AtLETM2 Affect Plant Viability—To characterize the function of *Arabidopsis* AtLETM proteins *in planta*, two independent knock-out lines were obtained for each gene, and the site of the T-DNA insertion was confirmed by DNA sequencing (Fig. 1*B*). Homozygous knock-out plants for each gene were obtained, and for single homozygous knock-out plants, shoot growth, leaf development, and flowering appeared normal (Fig. 1*C* and supplemental Fig. 1). Analysis of root growth on vertical MS plates revealed a noticeable reduction in root length of ~15% in *letm1* plants (supplemental Fig. 1*A*). Attempts to obtain double homozygous knock-out plants were not successful, and only plants that were homozygous knock-out for one of the *LETM* genes and hemizygous for the other could be obtained (Fig. 1*A*). It was noticed that there was a phenotypic difference in the hemizygous plants, which differed between which of the two *LETM* genes were present in hemizygous form in the genome. *LETM1*(+/−) *letm2*(−/−) displayed a normal phenotype, similar to any single homozygous knock-out (Fig. 1*A*). However, *letm1*(−/−) *LETM2*(+/−) plants consistently displayed retarded growth in the first few weeks after germination, with true leaves 1–6 showing irregular deformations (Fig. 1, *C* and *D*). Early root growth was severely impaired to only 40% of that in wild-type (Col-0) plants but improved to normal rates and length with age (supplemental Fig. 1*A*). Germination itself did not appear to be affected in any of the mutant lines. Leaves 1 and 2 (growth stage 1.02) emerged around day 10 in wild-type and single mutant plants, whereas true leaves in *LETM1*(+/−) *letm2*(−/−) plants emerged 2 days later (supplemental Fig. 1, *B* and *E*). Emergence of true leaves was delayed until leaf 6 (stage 1.06), after which no significant difference in emergence time could be observed with wild-type (Col-0) plants (supplemental Fig. 1, *B* and *F*). Similarly, morphological aberrations were observed in leaves 1–6, whereas leaves 7 and onward developed normally, similar to wild-type plants. The maximum rosette radius was 10–15% smaller in *LETM1*(+/−) *letm2*(−/−) plants until 30 days after sowing, upon which mutant plants caught up with wild-type (Col-0) plants (supplemental Fig. 1*C*). Thus, after 4 or more weeks, the plants appeared essentially normal. The appearance of the first open flower (stage 6.00) was marginally delayed by on average 1.5 days (supplemental Fig. 1*F*). It was also noticeable in the hemizygous *letm1*(−/−) *LETM2*(+/−) plants that the lesions at the leaf edges corresponded to where At*LETM1* was expressed, as determined by At*LETM1* promoter:GUS fusion (Fig. 1*E*).

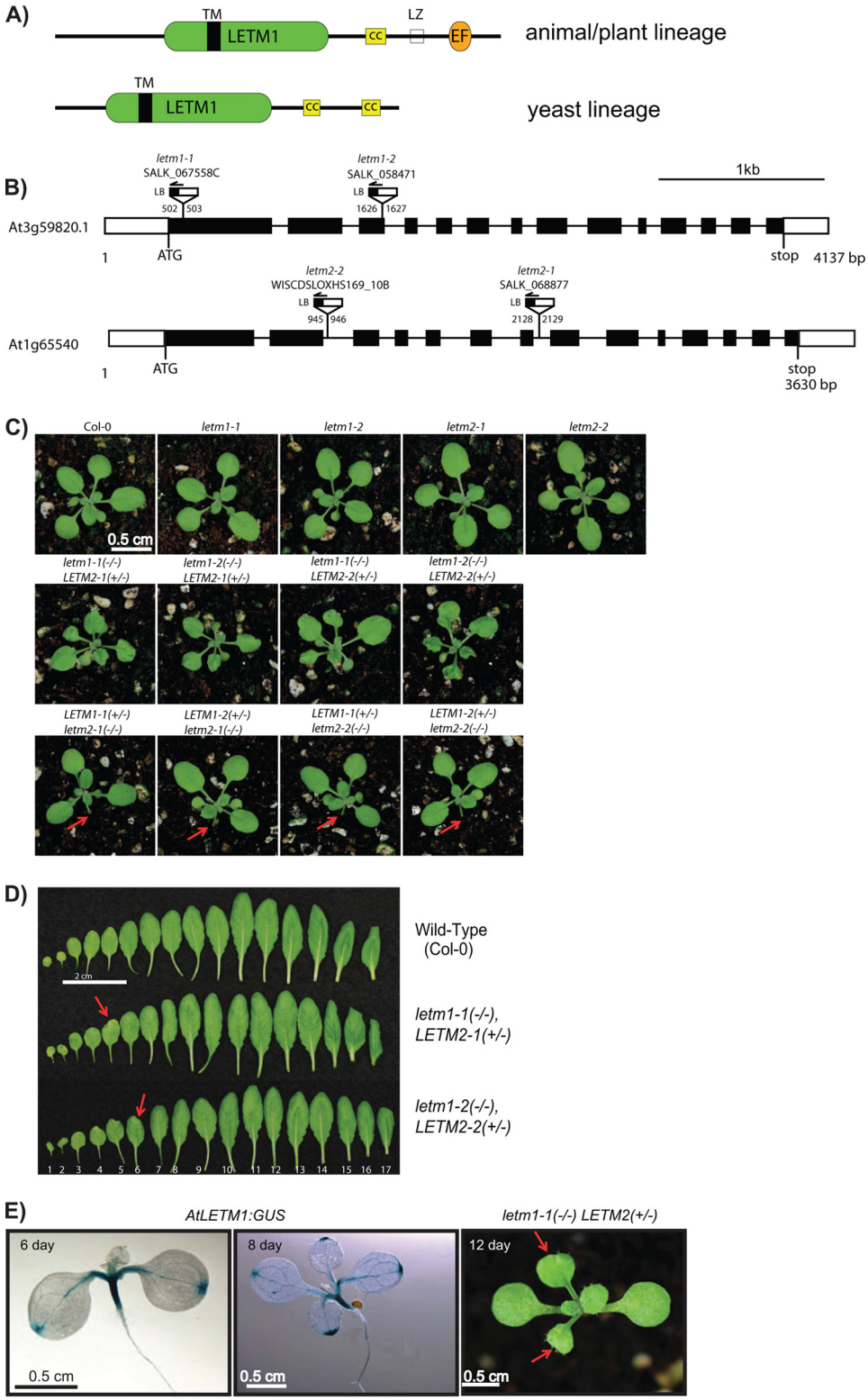

FIGURE 1. **Identification of *AtLETM1* and *AtLETM2* mutants.** *A*, diagram of the domain structure of LETM1-like proteins. *TM*, transmembrane region; *cc*, coiled-coil; *LZ*, leucine zipper; *EF*, EF-hand domain. *B*, diagram of insertion positions of T-DNAs in *AtLETM1* and *AtLETM2*. *Black boxes*, *open boxes*, and *black lines* indicate exons, untranslated regions, and introns, respectively. Insertion sites were verified by sequencing of PCR products. *C*, 18-day-old wild type (Col-0) and *AtLETM1* and *AtLETM2* single and double mutants grown under long day regime (16-h photoperiod). The *arrows* indicate the leaves harvested for genotyping. *D*, arrangement of cotyledons and leaves 1–12 of wild-type and hemizygous *letm1-1*(−/−) *LETM2-1*(+/−) plants. The *arrows* indicate deformations at the leaf edge of young leaves. *E*, comparison of 12-day-old mutant *letm1-1*(−/−) *LETM2-1*(+/−) plant with 6–8-day-old *AtLETM1* promoter-GUS reporter plants. The *arrows* indicate malformed leaf edges, which correspond with GUS the expression pattern.

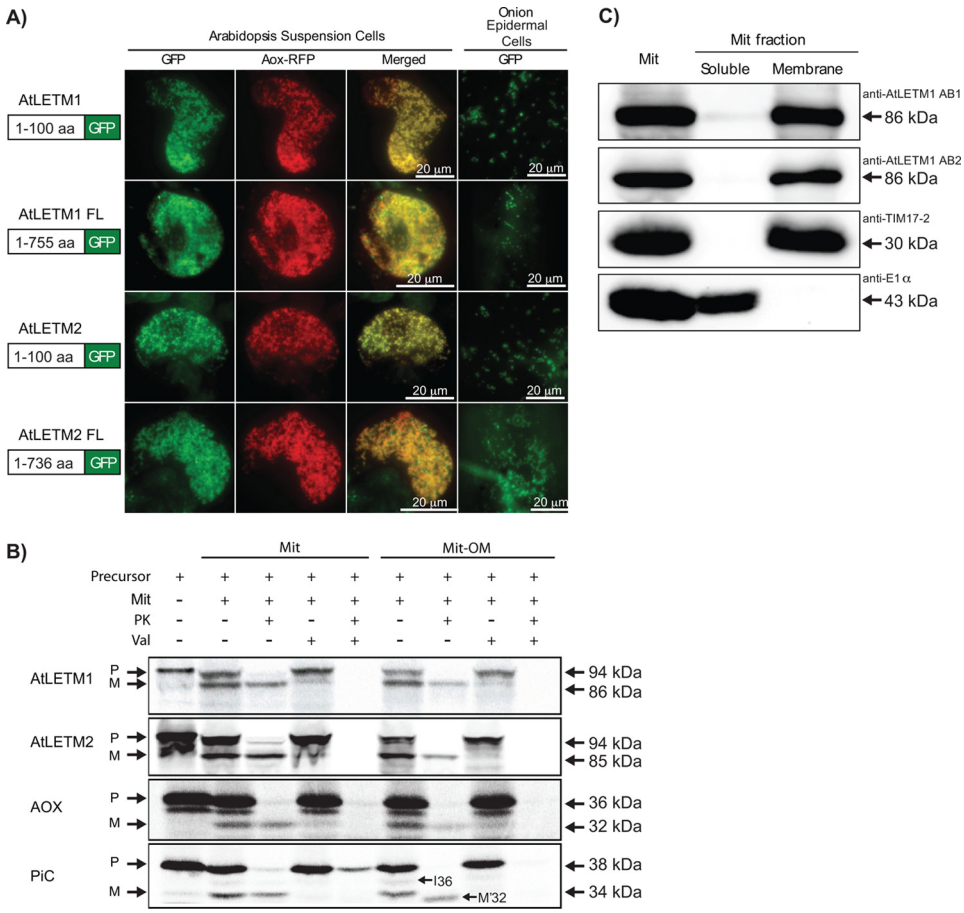

FIGURE 2. ***In vivo* and *in vitro* subcellular localization assay of AtLETM1 and AtLETM2.** *A*, the full length (*FL*) and first 100 N-terminal amino acids (*aa*) were fused to the N terminus of GFP to assess targeting of GFP. AOX-RFP was used as a mitochondrial marker. *Scale bars*, 20 μm. *B*, *in vitro* import of radiolabeled AtLETM1 and AtLETM2 into isolated mitochondria. The radiolabeled precursor proteins were incubated with mitochondria under conditions that support protein uptake into mitochondria. The uptake of the AOX from *Arabidopsis* and PiC from maize was used as a control for mitochondrial import. *Mit*, mitochondria; *Mit-OM*, mitochondria with the outer membrane ruptured; *PK*, proteinase K; *Val*, valinomycin; *P*, precursor protein band; *M*, inner membrane protected protein band; *I*, intermediate protein; *M′*, inner membrane protected mature band protein when the outer membrane was ruptured prior to protease treatment. *C*, Western blotting of isolated mitochondria of wild-type (Col-0) and mitochondrial soluble and membrane fractions extracted by sodium carbonate. Two antibodies raised against AtLETM1 (AtLETM1 AB1 and AtLETM1 AB2) and antibodies against TIM17-2 and pyruvate dehydrogenase E1α were used as controls for membrane and soluble proteins, respectively. The apparent molecular masses are indicated in kDa as calculated using an LMW calibration kit (GE Healthcare).

AtLETM1 and AtLETM2 Are Mitochondrial Inner Membrane Proteins—Although we have previously demonstrated that AtLETM1 is a mitochondrial protein (45), analysis of the targeting specificity for AtLETM2 was also carried out to confirm a mitochondrial location. Transient transformation of full-length AtLETM2 or the first 100-amino acid sequence of AtLETM2 coupled to GFP via the N terminus into *Arabidopsis* suspension cells or onion epidermal cells resulted in an exclusively mitochondrial pattern (Fig. 2*A*). In order to determine the intraorganellar location of AtLETM1 and AtLETM2, *in vitro* import assays were carried out (Fig. 2*B*). For this, radiolabeled full-length proteins were incubated with freshly isolated mitochondria. *In vitro* import of both AtLETM1 and AtLETM2 was observed, as evidenced by the appearance of a processed peptide designated the mature protein, using both intact mitochondria and mitochondria with the outer membrane removed. The processed peptide was protected against proteinase K degradation and required a membrane potential to cross the inner mitochondrial membrane, as shown by the lack of import in the presence of the transmembrane potential inhibitor, valinomycin. These results indicate that AtLETM1 and AtLETM2 proteins are imported into or across the inner mitochondrial membrane (Fig. 2*B*).

Antibodies were raised against two regions of AtLETM1 protein sequence (supplemental Fig. 2). Using full-length *in vitro* expressed AtLETM1 and AtLETM2 proteins, it was demonstrated that the AtLETM1 antibody 1 (AtLETM1 AB1) cross-reacted with both AtLETM1 and AtLETM2 proteins, whereas AtLETM1 antibody 2 (AtLETM1 AB2) only cross-reacted with AtLETM1 (supplemental Fig. 2*C*). Probing intact mitochondria along with membrane and soluble mitochondrial fractions, obtained using carbonate extractions from wild-type Col-0 plants, indicated that both AtLETM1 and AtLETM2 were uniquely located in the membrane fraction (Fig. 2*C*). These results taken together with the *in vitro* import assays demonstrate that AtLETM1 and AtLETM2 are mitochondrial inner membrane proteins, in agreement with the presence of a transmembrane domain (Fig. 1*B*). It is also worth noting that the absence of AtLETM1 could be clearly demonstrated in mitochondria from the *letm1-1*(−/−) *LETM2-1*(+/−) line because

probing mitochondria isolated from this line with both antibodies detected a specific product when probed with AtLETM1 AB1, but no product was detected when probed with AtLETM1 AB2 (supplemental Fig. 2*D*).

AtLETM1 or AtLETM2 Is Required for Efficient Translation in Mitochondria—To determine the reason for the early growth defect observed with *letm1*(−/−) *LETM2*(+/−) plants, a variety of assays characterizing mitochondrial function were carried out. Transmission electron microscopy analysis of mitochondria and crossing *letm1-1*(−/−) *LETM2-1*(+/−) plants stably transformed with GFP fused to a mitochondrial targeting signal (48) did not reveal any differences in morphology, number, or abundance of mitochondria (supplemental Fig. 3). However, it was apparent that chloroplast structure was altered in leaves in that there was a large accumulation of starch in the chloroplasts, and plastoglobules were noticeably larger (supplemental Fig. 3*A*). The increased accumulation of starch in *letm1*(−/−) *LETM2*(+/−) lines was confirmed with starch leaf stains carried out at the end of the light period and at the end of the dark period (supplemental Fig. 3*C*). Significantly more starch was apparent in the *letm1*(−/−) *LETM2*(+/−) plants compared with wild-type tissue. Notably, the accumulation and breakdown of starch in the cotyledons was unaffected and was similar to wild type (supplemental Fig. 3*C*).

Because hemizygous (*letm1-1*(−/−) *LETM2-1*(+/−)) plants still contain a functional *LETM* gene, the reason for the aberrant growth phenotype was investigated. Using antibodies raised against the LETM protein, Western blot analysis was carried out on mitochondria isolated from wild-type (Col-0) plants and each mutant allele, *letm1*(−/−) *LETM2*(+/+), *LETM1*(+/+) *letm2*(−/−), and hemizygous (*letm1-1*(−/−) *LETM2-1*(+/−)) (Fig. 3). Strikingly, mitochondria from hemizygous plants (*letm1-1*(−/−) *LETM2-1*(+/−)) contained half the amount of LETM protein compared with wild-type (Col-0) or when two alleles were present, *letm1*(−/−) *LETM2*(+/+) or *LETM1*(+/+) *letm2*(−/−) (Fig. 3*A*). Noticeably, *letm1*(−/−) *LETM2*(+/+) plants that displayed a mild root growth phenotype and had a slight reduction in the amount of LETM2 protein (supplemental Fig. 1*A*). The linearity of detection with the LETM antibody was demonstrated with dilution of mitochondrial protein (Fig. 3*A*). To investigate if the abundance of additional mitochondrial proteins was being modulated, Western blot analyses were carried out. It was revealed that the abundance of proteins in Complex I (NAD9), Complex III (RISP), and Complex IV (COX II) was not significantly changed compared with wild-type (Col-0). However, the α-subunit of ATP synthase (ATPα) was consistently reduced in abundance by almost 50% in hemizygous plants (Fig. 3*B*). To further investigate if any other mitochondrial processes were affected, Western blot analysis was carried out using antibodies to AOX, a stress-induced bypass component of the plant respiratory chain (49). AOX is induced by a variety of stresses, in particular perturbation of Complex I (50) and IV (51) of the cytochrome respiratory chain. There was no increase in abundance of AOX. Also, there was no increase in the amount of the mitochondrial uncoupling protein (Fig. 3*B*). Porin and TOM40 antibodies were used to verify equal protein loading (Fig. 3*B*).

Because yeast Mdm38 had been previously demonstrated to be required for the translation of *COXI* and *CYTB* (16), the rate of translation of proteins in mitochondria was investigated. Mitochondria were isolated from *Arabidopsis* seedlings, and *in organello* protein synthesis revealed that the translation of multiple proteins was reduced in mitochondria isolated from *letm1-1*(−/−) *LETM2-1*(+/−) mutant plants (Fig. 4*A*). Because over 50 proteins are encoded in the *Arabidopsis* mitochondrial genome (53), it is not possible to identify all protein bands based on apparent molecular mass; however, based on previous studies, six protein bands (namely ATPα, ATP9, NAD6 and -9, CYTB, and COXII) can be identified based on apparent molecular mass (10, 26). There was some decrease or increase observed in the single mutants, with translation in the single mutant *letm1*(−/−) *LETM2*(+/+) consistently displaying an approximately 10–20% reduction and translation in *LETM1(+/+) letm2(−/−)* displaying a 10–20% increase, with the exception of subunit 9 of ATP synthase, which was translated at the highest levels in wild type (Fig. 4*A*). Translation of subunit 9 in all mutants was reduced, but it was reduced by the greatest amount in the hemizygous mutant, where it reached 35% of wild-type levels (Fig. 4*A*). It was notable that the difference in incorporation of [^{35}S]Met into protein was greatest after 60 min, with significant differences ($p < 0.01$, Student's *t* test) between incorporation from mitochondria from Col-0 and *letm1-1*(−/−) *LETM2-1*(+/−) observed for all proteins. However, after 10 min, little or no incorporation was detected, and after 30 min, the difference in incorporation of [^{35}S]Met for ATPα and CYTB was not significant (Fig. 3*A*). Thus, the differences were most apparent after 60 min.

Analysis of the incorporation of [^{35}S]methionine into ATP9, compared with incorporation into the other protein bands that could be identified revealed that it accounted for >50% of incorporation of [^{35}S]Met in mitochondria from wild-type plants (supplemental Fig. 4). Note that although the incorporation of [^{35}S]Met was still 42% into ATP9 in mitochondria from hemizygous *letm1-1*(−/−) *LETM2-1*(+/−) plants, incorporation into ATP9 was only one-third compared with wild type. Thus, Western blot analysis showed that the steady state abundance of the α-subunit of ATP synthase decreases in mitochondria from *letm1-1*(−/−) *LETM2-1*(+/−) plants compared with the other genotypes; *in organelle* translation indicated that the translation of all mitochondrial products detected by SDS-PAGE was affected in the *letm1-1*(−/−) *LETM2-1*(+/−) hemizygous background and that the greatest reduction was observed with ATP9, but the translation of ATPα was also reduced by almost 50% in mitochondria from *letm1-1*(−/−) *LETM2-1*(+/−) plants.

To investigate this further, mitochondria from Col-0, *letm1*(−/−) *LETM2*(+/+), *LETM1*(+/+) *letm2*(−/−), and hemizygous (*letm1-1*(−/−) *LETM2-1*(+/−) plants were analyzed by BN-PAGE to determine any differences in pattern and abundance (Fig. 4*B*). It was apparent that upon examination of the Coomassie-stained gel, the mitochondria from Col-0, *letm1*(−/−) *LETM2*(+/+), and *LETM1*(+/+) *letm2*(−/−) displayed the same pattern of protein complexes, but mitochondria from hemizygous *letm1-1*(−/−) *LETM2-1*(+/−) plants had a relative decrease in the amount of Complex V and

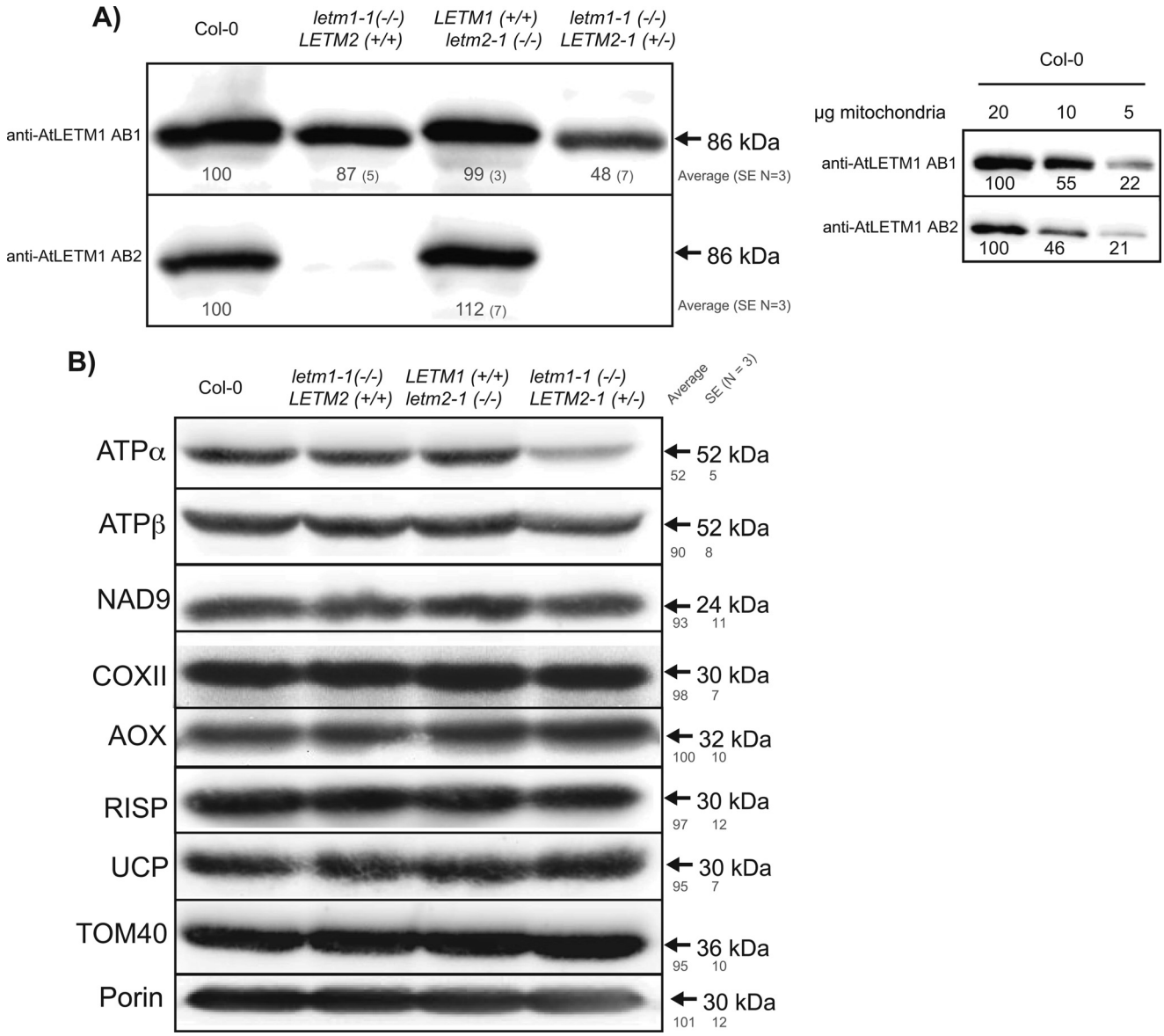

FIGURE 3. **Analysis of mitochondrial protein abundance.** *A*, Western blot analysis of mitochondria isolated from 10-day-old plants of wild-type (Col-0), *letm1*(−/−) *LETM2*(+/+), *LETM1*(+/+) *letm2*(−/−), and *letm1*(−/−) *LETM2*(+/−) with antibodies raised against LETM1. Equal amounts of mitochondrial protein were loaded in each lane. Dilutions of mitochondrial proteins from 20 to 5 μg were separated by SDS-PAGE, blotted to supported nitrocellulose, and probed with the LETM1 antibody. Detection of cross-reacting products was carried out using chemiluminescence, and the signal was captured using ImageQuant RT ECL (GE Healthcare) with the signal intensity (pixel intensity) adjusted relative to wild type (Col-0) and set to 100. *Numbers* in *gray* represent intensity with S.E. from $n = 3$. *B*, mitochondria from 10-day-old water culture-grown plants were isolated and separated by SDS-PAGE and probed with antibodies to a variety of mitochondrial proteins. The change in abundance of protein in the *letm1-1*(−/−) *LETM2-1*(+/−) line compared with wild type (Col-0) is indicated *beside* each blot with S.E. values. *UCP*, uncoupling protein; RISP, Rieske FeS protein.

an increase in a distinct band with an apparent molecular mass of ~800 kDa (Fig. 4*B*). To verify the identity of these bands, mass spectrometry was utilized, confirming that the band that decreased in intensity was Complex V, with the β-subunit and subunit 8 of ATP synthase identified from an excised band (Fig. 4*B* and supplemental Table 2). The band that increased in abundance in mitochondria from hemizygous *letm1-1*(−/−) *LETM2-1*(+/−) contained the α- and β-subunit of ATP synthase, HSP60-2, HSP60-3B ATP/ADP carrier 2, ORF25 (which encodes a subunit of ATP synthase (54)), and ATP synthase D subunit (Fig. 4*B* and supplemental Table 2). Biochemical assays indicated that the oxidation of NADH, pyruvate, and malate were not significantly different between wild-type and hemizygous *letm1-1*(−/−) *LETM2-1*(+/−). Although succinate oxidation appeared to be lower with intact mitochondria, determination of succinate dehydrogenase activity in isolated mitochondria revealed almost identical values (Fig. 4*C*). Because both the Western blot analysis and BN-PAGE indicated that the abundance of ATP synthase was decreased, ATP level in leaves were measured and observed to be reduced by 50% (Fig. 4*C*).

To investigate if any other processes were affected in the hemizygous (*letm1-1*(−/−) *LETM2-1*(+/−)) plants, protein import rates of AOX and PiC into isolated mitochondria and transcript abundance of mitochondrially encoded genes were measured (Fig. 5). *In vitro* import assays with the precursors of

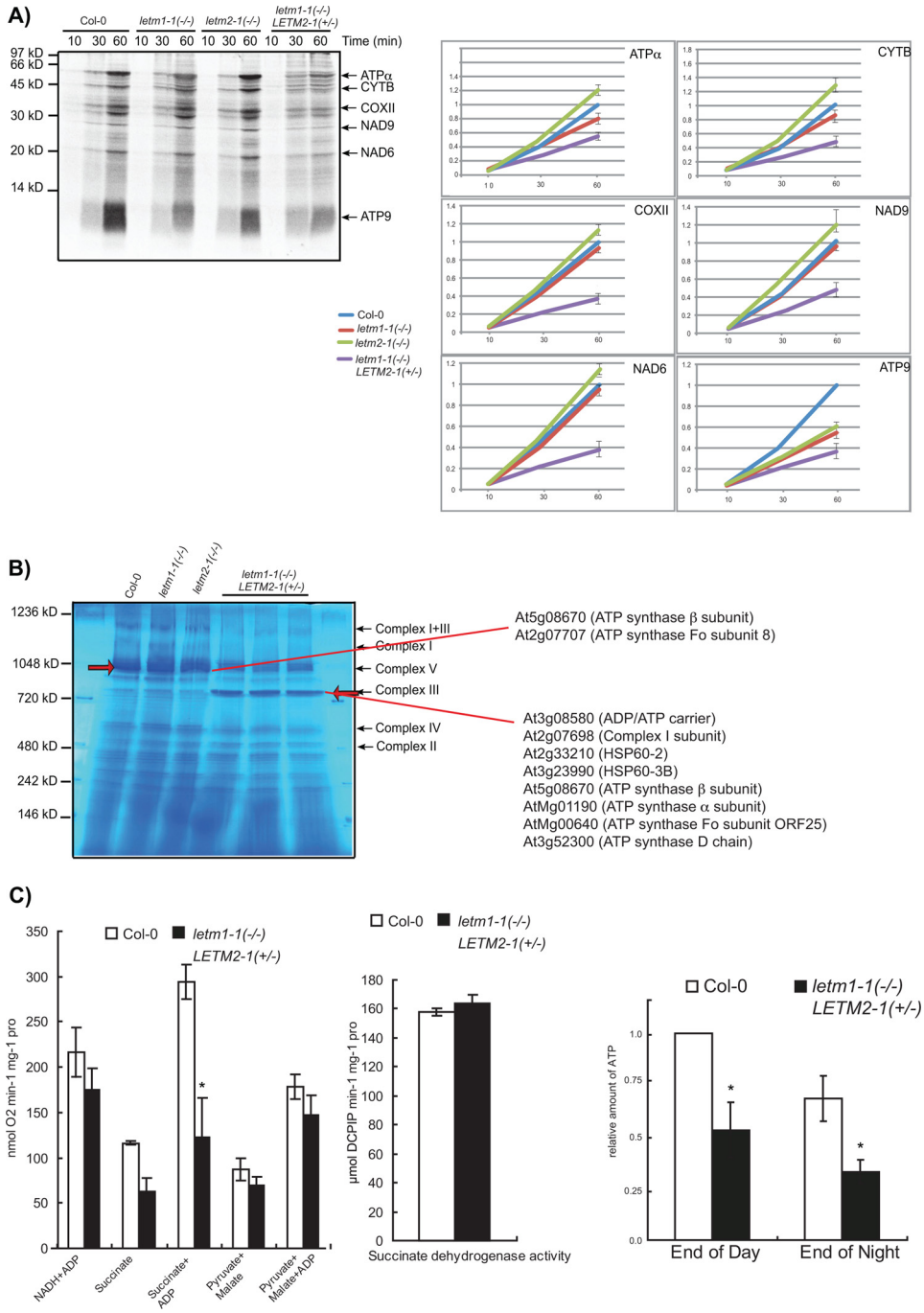

FIGURE 4. **Analysis of mitochondrial proteins in *letm1*(−/−) *LETM2*(+/−) plants.** *A*, *in organello* protein synthesis in mitochondria isolated from 10-day-old plants of wild-type (Col-0), *letm1*(−/−) *LETM2*(+/+), *LETM1*(+/+) *letm2*(−/−), and *letm1*(−/−) *LETM2*(+/−) plants analyzed by SDS-PAGE. Shown is incorporation of [^{35}S]methionine into proteins from mitochondria isolated from wild-type (Col-0), *letm1*(−/−) *LETM2*(+/+), *LETM1*(+/+) *letm2*(−/−), and *letm1*(−/−) *LETM2*(+/−) plants. The *arrows* indicate bands that can be identified from their apparent molecular mass based on previous studies (10, 20), and incorporation of [^{35}S]methionine into these bands was determined over time. *B*, BN-PAGE analysis of mitochondrial proteins isolated from 10-day-old plants of wild type (Col-0), *letm1*(−/−) *LETM2*(+/+), *LETM1*(+/+) *letm2*(−/−), and *letm1*(−/−) *LETM2*(+/−). The *red arrows* indicate the bands that were different between wild type (Col-0), *letm1*(−/−) *LETM2*(+/+), *LETM1*(+/+) *letm2*(−/−), and *letm1*(−/−) *LETM2*(+/−), and these bands were subject to mass spectrometry for identification. *C*, oxygen consumption of mitochondria isolated from wild type (Col-0) and hemizygous *letm1-1*(−/−) *LETM2-1*(+/−) plants in the presence of different substrates. Succinate dehydrogenase activity in wild-type (Col-0) and hemizygous *letm1-1*(−/−) *LETM2-1*(+/−) plants. Shown is measurement of total ATP content of leaves from wild-type (Col-0) and hemizygous *letm1-1*(−/−) *LETM2-1*(+/−) plants. The amount of ATP is normalized to the highest amount measured in wild type (Col-0). *Error bars*, S.E.

AOX and PiC revealed no significant differences in import rate over time. For AOX, which is imported via the general import pathway, import increased over time, as judged by protection from externally added protease (Fig. 5*A*). In the case of PiC, which is imported by the carrier import pathway, import was observed to increase over time, where initial protease protection of the precursor was evident, representing stage III of the carrier import pathway (55), and this was converted to the mature protein over time (Fig. 5*A*, *M*). A weak intermediate band was also observed (Fig. 5*A*, *I*) because this carrier protein

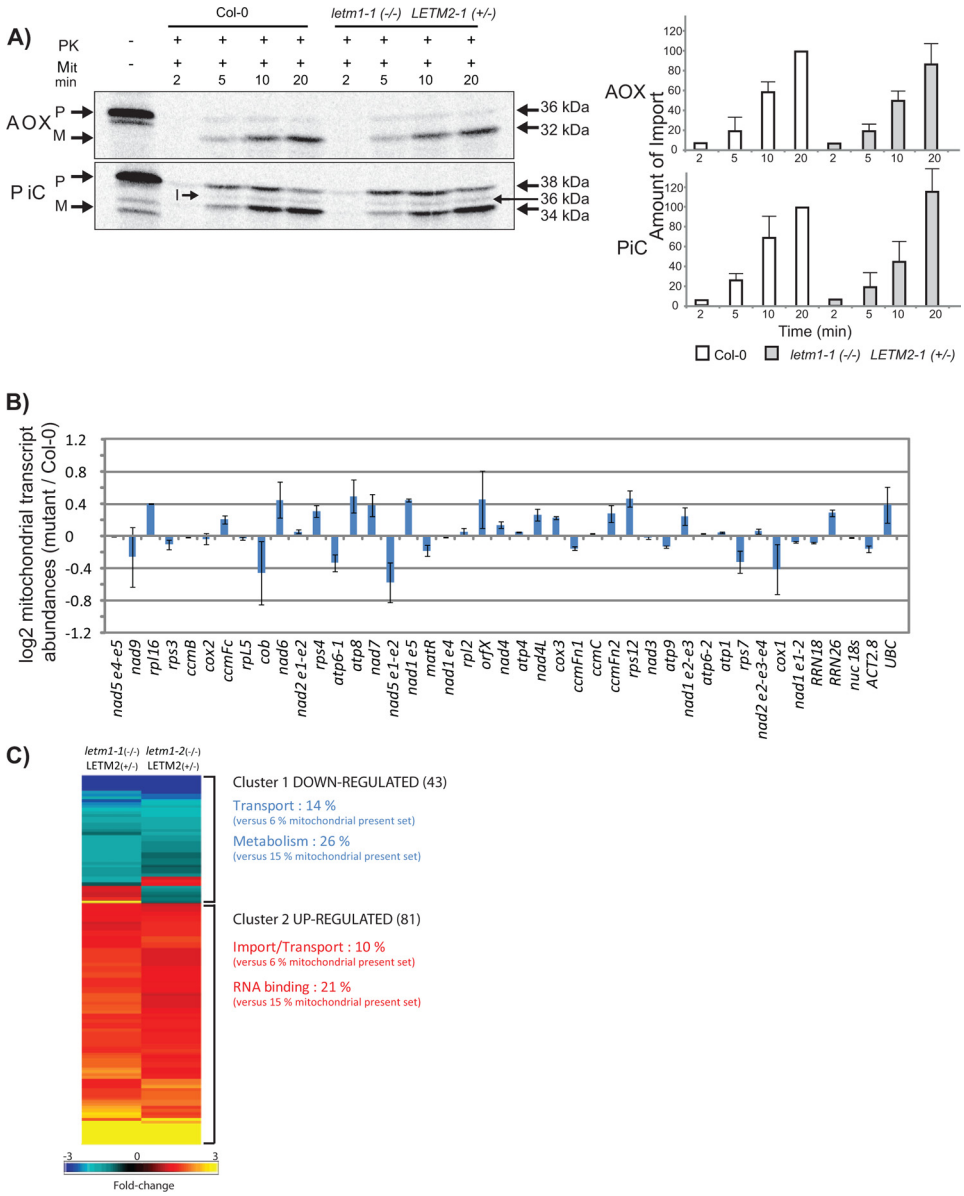

FIGURE 5. **Analysis of the import of proteins and steady state mitochondrial transcript abundance levels in *letm1-1*(−/−) *LETM2-1*(+/−) *Arabidopsis* plants.** *A*, import of PiC and AOX into isolated mitochondria from 10-day-old wild-type (Col-0) and *letm1-1*(−/−) *LETM2-1*(+/−) mutant in liquid culture. Radiolabeled translation products were incubated with isolated mitochondria, and samples were taken at different time intervals. Protein extracts were then separated by SDS-PAGE. The precursor (*P*), mature (*M*), and intermediate (*I*) bands and the addition of externally added protease (*PK*) are indicated. The rate of import was quantified from three individual mitochondrial isolations, and the average and S.E. values (*error bars*) ($n = 3$) are shown. *B*, quantitative RT-PCR was carried out to determine the abundance of mitochondrial transcripts in *letm1-1*(−/−) *LETM2-1*(+/−) mutant seedlings compared with wild-type (Col-0) seedlings. Transcript abundance is displayed as $\log_2$ of the ratio of values determined in mutant *versus* wild-type (Col-0) samples for each transcript. Three biological replicates were performed, with three technical replicates for each sample performed and averaged; S.E. values are indicated. Nuclear *18S* (used as a normalization control) along with *ACT2* and *UBC* transcripts were included as controls. *C*, summary of differentially expressed genes with -fold changes greater than 1.5-fold, after false discovery rate correction, either up-regulated (shown in *red shading*) or down-regulated (shown in *blue shading*) for various comparisons between different genotypes. A *color scale* is shown. *Brighter red* and *blue coloring* and *black boxes* indicate that a greater number of transcripts are changing in *letm1*(−/−) *LETM2*(+/−) *versus* wild-type (Col-0) plants.

contains a cleavable presequence that is processed in two steps (29). Analysis of transcript abundance for mitochondrially encoded transcripts revealed no significant change. Notably, no changes were detected in the transcript abundance of ATPα. Finally, the transcript abundance of nucleus-encoded genes was measured using microarray analysis. Analysis of transcript levels for 1202 nuclear genes encoding mitochondrial proteins (48) revealed that only 10% (124) of these genes were altered in abundance by more than 1.5-fold in either of the *letm1*(−/−) *LETM2*(+/−) lines compared with Col-0 (supplemental Table 3). Furthermore, only six and eight mitochondrial components were down- or up-regulated, respectively, by 2-fold or more in both *letm1-1*(−/−) *LETM2*(+/−) and *letm1–2*(−/−) *LETM2*(+/−) lines based on global transcript abundances, indicating very minor reprogramming in regard to mitochondrial metabolism (supplemental Table 3 and Fig. 5*C*). Functional categorization analysis of both the up- and down-regulated transcripts encoding mitochondrial proteins revealed an overrepresentation of import and RNA binding-related functions in up-regulated transcripts, whereas transcripts encoding

proteins with transport and metabolism functions were over-represented in the down-regulated transcripts (Fig. 5*C*). This is consistent with a general role for the involvement of AtLETM in translation, with a reduction in AtLETM protein abundance compensated for by the induction of other RNA-binding proteins as a possible mechanism to stabilize transcripts from degradation. The lack of induction of a variety of transcripts encoding mitochondrial proteins is consistent with the lack of significant changes of protein abundances in Complex I, III, IV or the respiratory chain, as revealed by Western blotting.

letm2 Exhibits Maternal Effect Seed Abortion—Analysis of developing seeds within the siliques of hemizygous *letm1*(−/−) *LETM2*(+/−) self-fertilized mutants revealed that half of the developing seeds were aborted (Fig. 6*A* and supplemental Table 4). To examine whether the *LETM2* gene is required for the development of the female gametophyte, we inspected unpollinated ovules. In *Arabidopsis*, the mature embryo sac consists of an egg cell, a central cell, two synergid cells, and three degenerated antipodal cells (57–59). Morphologically, embryo sac development in ovules of *letm1*(−/−) *LETM2*(+/−) plants was indistinguishable from wild type (Fig. 6*B*, *1* and *5*). Whole-mount preparations of ovules 12–60 h after pollination revealed that more than 90% of the embryo sacs had initiated embryo and endosperm development in the heterozygous mutants *letm1*(−/−) *LETM2*(+/−), and during early embryogenesis (12–16 h after pollination) there was no difference between the developing seeds within the hemizygous siliques (Fig. 6*B*, *2* and *6*). However, embryo and endosperm were aborted at later stages of development in 50% of the seeds (Fig. 6, *A* and *B*, and supplemental Table 4). Among the aborted seeds, an apparently random proportion (supplemental Table 4) were arrested at quadrant/octant embryo stage with an endosperm arrested even earlier (Fig. 6*B*, *7*). At quadrant/octant embryo stage, the non-aborted seeds contained 36–48 ± 12 endosperm nuclei ($n = 10$), whereas aborted seeds had only 10–16 ± 5 nuclei ($n = 10$). Another proportion of the aborted seeds (supplemental Table 4) were arrested at early heart embryo stage (Fig. 3*B*, *8*) with an endosperm of 78–90 ± 11 nuclei ($n = 10$) as opposed to non-arrested seeds, which had 188–194 ± 8 endosperm nuclei ($n = 10$) at that stage.

Because 50% seed abortion is a strong indication for a defect that is under gametophytic control, we performed reciprocal crosses between *letm1*(−/−) *LETM2*(+/−) and *letm1*(−/−) *LETM2*(+/+) plants. When *letm1*(−/−) *LETM2*(+/−) plants were used as female, the *letm1*(−/−) *LETM2*(+/−) seed phenotype could not be complemented by fertilization with a wild-type *LETM2* allele derived from the pollen in ~50% of the F_1 seeds (Fig. 6*A*). Genotyping revealed that all viable seeds from this cross (239 of 239; Table 1) gave rise to *letm1*(−/−) *LETM2*(+/+) plants. In contrast, using maternal *letm1*(−/−) *LETM2*(+/+) in a cross with *letm1*(−/−) *LETM2*(+/−) did not impair seed development (Fig. 6*A* and supplemental Table 4), resulting in 100% viable seeds. F_1 plants from this cross displayed ~1.7:1 segregation of the *letm1-1*(−/−) *LETM2-1*(+/+) and *letm1*(−/−) *LETM2*(+/−) genotypes (271 and 155 individuals, respectively; Table 1). This segregation ratio is significantly different from the expected 1:1 ratio ($p < 0.005$), indicating that pollen with the genotype *letm1*(−) *letm2*(−) is viable yet slightly less fertile than *letm1*(−) *LETM2*(+) or wild-type pollen. When crossing *letm1*(−/−) *LETM2*(+/−) with Col-0, 100% seed viability was observed in either direction. However, genotyping of the F_1 progeny indicated that using paternal Col-0 showed 1:1 (124:116 individuals; Table 1) *LETM1*(+/−) *LETM2*(+/+) *versus LETM1*(+/−) *LETM2*(+/−) segregation, whereas using paternal *letm1*(−/−) *LETM2*(+/−) resulted in ~1.6:1 (146:94 individuals) *LETM1*(+/−) *LETM2*(+/+) *versus LETM1*(+/−) *LETM2*(+/−) segregation. This segregation ratio is also significantly different from the expected 1:1 ratio ($p < 0.005$). Pollen viability and number were assessed using the Alexander staining method (Fig. 6*C*) (38). A slight increase in defective pollen was observed in pollen of *letm1*(−/−) *LETM2*(+/−) plants compared with Col-0. *letm1*(−/−) *LETM2*(+/−) flowers produced ~60% less pollen than Col-0. Again, these observations suggest that pollen with genotype *letm1*(−) and *letm2*(−) is viable yet slightly less fertile than *letm1*(−) *LETM2*(+) or wild-type pollen. Similar results were obtained using independent alleles for all mutations.

The parent of origin effect on seed viability observed with the *letm2* mutant could be due to a requirement for LETM2 protein during female gametophyte development or due to only the maternal allele being expressed during seed development. To investigate the maternal expression of *LETM2*, we performed reciprocal crosses of the *LETM2*::*GUS* promoter reporter lines with Col-0 plants (Fig. 7, *A* and *B*). Although there is some loss of cellular resolution due to the staining procedure, a phenomenon that is routinely observed (37, 60, 61), GUS expression under the control of the *AtLETM2* promoter is observed in the female gametophyte and in developing seed (Fig. 7*A*). When using the *LETM2*::*GUS* promoter reporter line as a female in a cross with Col-0, GUS expression was observed (Fig. 7*B*). However, when using the *LETM2*::*GUS* promoter reporter line as male, no GUS activity was observed (Fig. 7*B*). Notably, in a similar experiment using the *AtLETM1* promoter, no GUS expression was observed in endosperm or embryo, consistent with previous findings that AtLETM1 is stress-induced (45).

Furthermore, we dissected 6-day-old seeds of reciprocal crosses between Col-0 and L*er* plants and isolated embryo and endosperm tissues for transcript sequencing. The T to C polymorphism between Col-0 and L*er* in the mRNA sequence of *LETM2* allowed differentiation of transcripts originating from the Col-0 or L*er* allele. As a control, a 1:1 mix of Col-0 and L*er* cDNA was used, and as expected, this cDNA showed equal amounts of each polymorphism in the chromatograms (Fig. 7*C*). Analysis of the Col-0 × L*er* crosses revealed a clear abundance of the maternal transcript in both embryo and endosperm (Fig. 7*C*). Thus, seed viability depends only upon the presence of a wild-type maternal *LETM2* allele.

DISCUSSION

This study has defined the overlapping functions performed by AtLETM1 and AtLETM2 as essential for mitochondrial function and viability. Mechanistically, LETM function was defined as being important for accumulation of mitochondrial

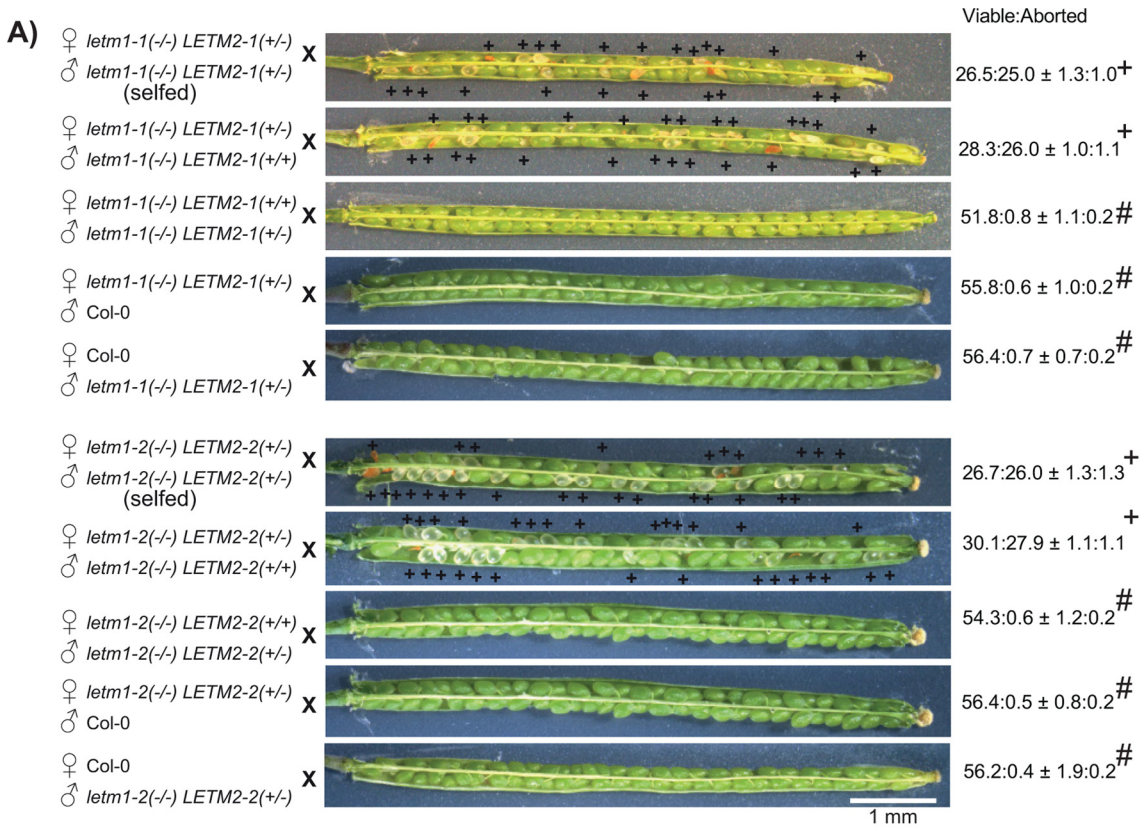
A)
Viable:Aborted
♀ letm1-1(-/-) LETM2-1(+/-)
♂ letm1-1(-/-) LETM2-1(+/-)
(selfed)
X
26.5:25.0 ± 1.3:1.0+
♀ letm1-1(-/-) LETM2-1(+/-)
♂ letm1-1(-/-) LETM2-1(+/+)
X
28.3:26.0 ± 1.0:1.1+
♀ letm1-1(-/-) LETM2-1(+/+)
♂ letm1-1(-/-) LETM2-1(+/-)
X
51.8:0.8 ± 1.1:0.2#
♀ letm1-1(-/-) LETM2-1(+/-)
♂ Col-0
X
55.8:0.6 ± 1.0:0.2#
♀ Col-0
♂ letm1-1(-/-) LETM2-1(+/-)
X
56.4:0.7 ± 0.7:0.2#
♀ letm1-2(-/-) LETM2-2(+/-)
♂ letm1-2(-/-) LETM2-2(+/-)
(selfed)
X
26.7:26.0 ± 1.3:1.3+
♀ letm1-2(-/-) LETM2-2(+/-)
♂ letm1-2(-/-) LETM2-2(+/+)
X
30.1:27.9 ± 1.1:1.1+
♀ letm1-2(-/-) LETM2-2(+/+)
♂ letm1-2(-/-) LETM2-2(+/-)
X
54.3:0.6 ± 1.2:0.2#
♀ letm1-2(-/-) LETM2-2(+/-)
♂ Col-0
X
56.4:0.5 ± 0.8:0.2#
♀ Col-0
♂ letm1-2(-/-) LETM2-2(+/-)
X
56.2:0.4 ± 1.9:0.2#
1 mm

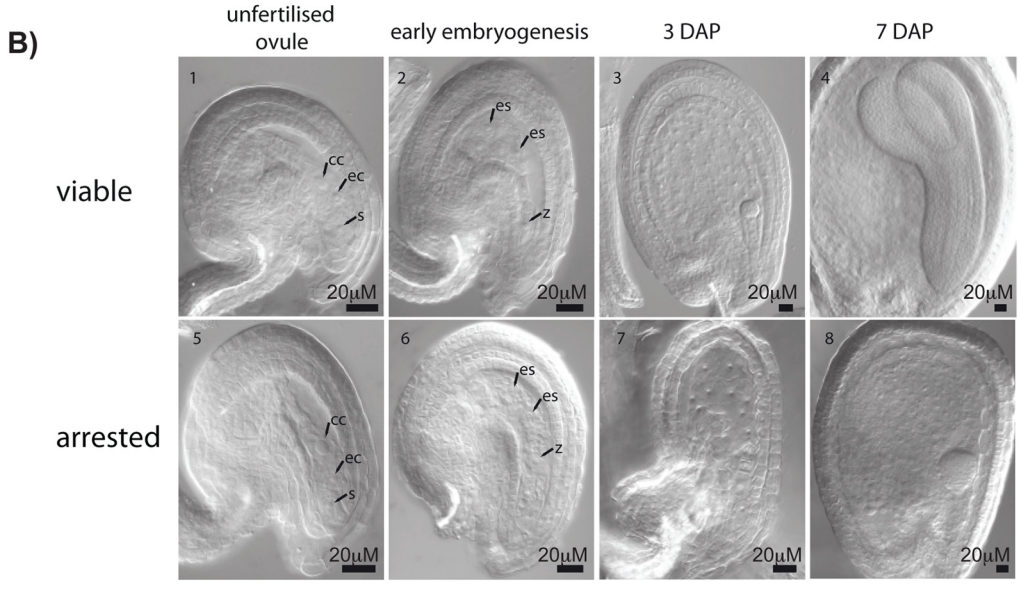
B)
unfertilised ovule
early embryogenesis
3 DAP
7 DAP
viable
arrested
1
2
3
4
5
6
7
8
cc
ec
s
es
z
20μM

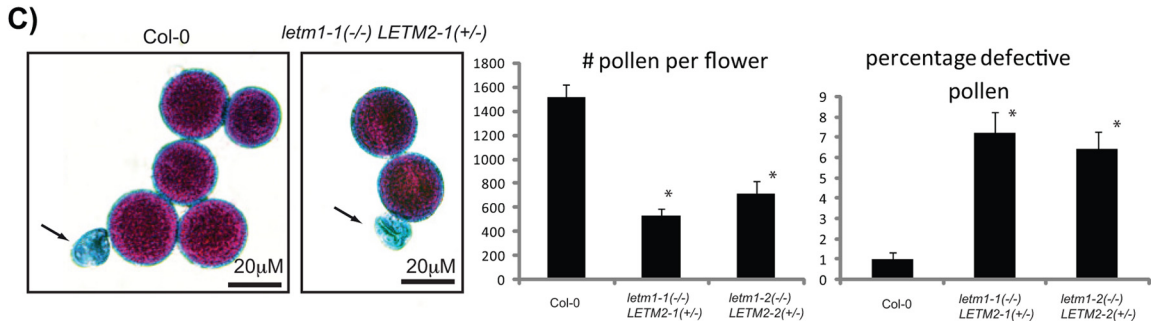
C)
Col-0
letm1-1(-/-) LETM2-1(+/-)
20μM
pollen per flower
percentage defective pollen
Col-0
letm1-1(-/-) LETM2-1(+/-)
letm1-2(-/-) LETM2-2(+/-)

TABLE 1

PCR genotyping of LETM crosses in the F_1 progeny

Reciprocal crosses were performed between different combinations of Col-0 and LETM mutant genotypes. The genotype of the F_1 progeny was determined using PCR-based genotyping.

Parents	F_1 progeny	Ratio
♀ *letm1-1(−/−)* × ♂ *letm1-1(−/−)* LETM2-1(+/−)	*letm1-1 (−/−)* LETM2-1 (+/+): *letm1-1 (−/−)* LETM2-1 (+/−)	149:81
♀ *letm1-1(−/−)* LETM2-1(+/−) × ♂ *letm1-1(−/−)*	*letm1-1 (−/−)* LETM2-1 (+/+): *letm1-1 (−/−)* LETM2-1 (+/−)	239:0
♀ *letm1-1(−/−)* LETM2-1(+/−) × ♂ Col-0	LETM1-1 (+/−) LETM2-1 (+/+): LETM1-1 (+/−) LETM2-1 (+/−)	59:61
♀ Col-0 × ♂ *letm1-1(−/−)* LETM2-1(+/−)	LETM1-1 (+/−) LETM2-1 (+/+): LETM1-1 (+/−) LETM2-1 (+/−)	73:47
♀ *letm1-2(−/−)* × ♂ *letm1-2(−/−)* LETM2-2(+/−)	*letm1-2 (−/−)* LETM2-2 (+/+): *letm1-2 (−/−)* LETM2-2 (+/−)	122:74
♀ *letm1-2(−/−)* LETM2-2(+/−) × ♂ *letm1-2(−/−)*	*letm1-2 (−/−)* LETM2-2 (+/+): *letm1-2 (−/−)* LETM2-2 (+/−)	208:0
♀ *letm1-2(−/−)* LETM2-2(+/−) × ♂ Col-0	LETM1-2 (+/−) LETM2-2 (+/+): LETM1-2 (+/−) LETM2-2 (+/−)	65:55
♀ Col-0 × ♂ *letm1-2(−/−)* LETM2-2(+/−)	LETM1-2 (+/−) LETM2-2 (+/+): LETM1-2 (+/−) LETM2-2 (+/−)	73:47

proteins. Although the translation of potentially all mitochondrial proteins was reduced in the hemizygous *letm1*(−/−) *LETM2*(+/−) plants, only the steady state level of ATP synthase was reduced, as determined by both Western blot analysis and BN-PAGE. Also the amount of ATP was reduced on a tissue basis, consistent with the decrease in the amount of ATP synthase. Note that although Western blot analysis revealed a reduction in the amount of ATPα, other subunits of this complex are also likely to be reduced in abundance, but there are no specific antibodies available for other subunits, apart from the β-subunit, which was not decreased in abundance. No evidence was found for a reduction in abundance of the other respiratory chain complexes, despite the fact that Complex I, III, and IV all contain mitochondrially encoded subunits, where the rate of translation was also reduced. It is proposed that this is due to the fact that mitochondrial biogenesis takes place during early development in plants; a directed study revealed that mitochondrial transcription and translation were the earliest mitochondrial events that could be detected after imbibition during germination (48). Second, the abundance of the ATP synthase complex can be seen to be greater than the other respiratory complexes that contain mitochondrially encoded subunits (Fig. 4*B*), and in general, the abundance of the ATP synthase complex is the highest of the respiratory chain complexes in isolated plant mitochondria, as evidenced by staining with Coomassie Brilliant Blue (62, 63). Furthermore, the incorporation of [^{35}S]Met into ATP9 represented >50% of the incorporated methionine in mitochondria from the six bands identified from Col-0 plants. ATP9 is present at a stoichiometry of 10 copies in yeast and mammalian mitochondria and thus contains 10 times more subunit 9 than subunit 6 or 8 (64). Consistent with our observation, the incorporation of radiolabeled methionine into ATP9 in yeast is also severalfold greater than other ATP synthase subunits (64). Five subunits of the ATP synthase are encoded in the mitochondrial genome of *Arabidopsis*: four subunits of the F_0 (namely orfB, orf25, subunit 6, and subunit 9) (54) and ATPα in F_1 (53). Thus, it is proposed that during the rapid burst of mitochondrial biogenesis that occurs early in germination, the rate of synthesis of the ATP synthase subunits is rate-limiting for assembly and thus is reduced in abundance compared with mitochondria from wild-type plants. This is especially relevant for the F_0 module, where subunit 9 is proposed as the initiating event for assembly of the F_0 module (64). Although the reduction in the accumulation of the mitochondrial ATP synthase does not lead to any detectable changes in mitochondrial morphology, notably there was an increased in starch and plastoglobule accumulation in chloroplasts. This is proposed to be due to the fact that a reduced mitochondrial ATP synthase results in an inability to respire all of the carbon that is fixed in photosynthesis, and it accumulates in storage products.

However, for the other respiratory chain complexes that contain mitochondrial encoded subunits, the rate of synthesis is not limiting, and thus no differences are observed in steady state abundance. This is also consistent with the fact that the phenotype is only observed early in development, where mitochondrial biogenesis peaks, and later even the reduced rate of synthesis is sufficient for these plants to achieve a normal phenotype. Additionally, the fact that the alternative respiratory chain is not induced, because the reduction in the ATP synthase leads to a reduction in the amount of ATP and thus induction of a non-phosphorylating bypass pathway, would not alleviate this biochemical lesion. Recently, an RNAi approach to reduce the abundance of the nucleus-encoded δ-subunit of ATP synthase also observed a defect in pollen formation, consistent with the finding in this study that the ATP synthase is critical for pollen development (65). Finally, although the abundance of Complex I, II, III, and IV was not reduced, despite the decrease in the rate of translation, it may also indicate that the rate of degradation of these complexes or subunits in these complexes can be adjusted, so that steady state abundance is unaffected. However for the ATP synthase, if the rate of degradation was adjusted, it cannot compensate for the reduced rate of synthesis. Because the difference in incorporation of [^{35}S]Met into protein was observed to be greatest after 60 min and much less at 30 min, it is possible

FIGURE 6. **Seed sets of crossing of *AtLETM1* and *AtLETM2* single and double mutants.** *A*, siliques from the self-crossing of double mutant *letm1-1*(−/−) *LETM2-1*(+/−) and the crossing of double mutant *letm1-1*(−/−) *LETM2-1*(+/−) with single mutant *letm1-1*(−/−) *LETM2-1*(+/+) and with wild-type (Col-0). +, aborted embryos. Values indicate the average number of viable and aborted progeny per silique ± S.D. ($n = 10$). *Scale bar*, 0.5 cm. The crosses of both alleles are shown, with the *top five panels* representing one allele of AtLETM1 and AtLETM2 and the *bottom five panels* representing similar crosses with the second allele for both AtLETM1 and AtLETM2. +, statistically similar to theoretical 1:1 ratio ($p > 0.50$); #, statistically similar to theoretical 1:0 ratio ($p > 0.90$). *B*, microscopic analysis of different stages of development for embryos in *letm1*(−/−) *LETM2*(+/−) mutant plants. Gametophyte, early embryo, and seeds 3 and 7 days after pollination (*DAP*) are shown. Some embryos of *letm1-1*(−/−) *LETM2-1*(+/−) plants are aborted in the 2–4-cell stage (*7*), whereas other embryos are aborted at the globular stage (*8*). *cc*, central cell; *ec*, egg cell; *s*, synergid; *es*, endosperm; *z*, zygote. *C*, number of pollen grains and percentage of defective pollen as determined by Alexander staining. *Arrow*, defective pollen grain. *, statistically significant difference compared with wild-type (Col-0) ($p < 0.01$). *Scale bars*, 20 μm. *Error bars*, S.E.

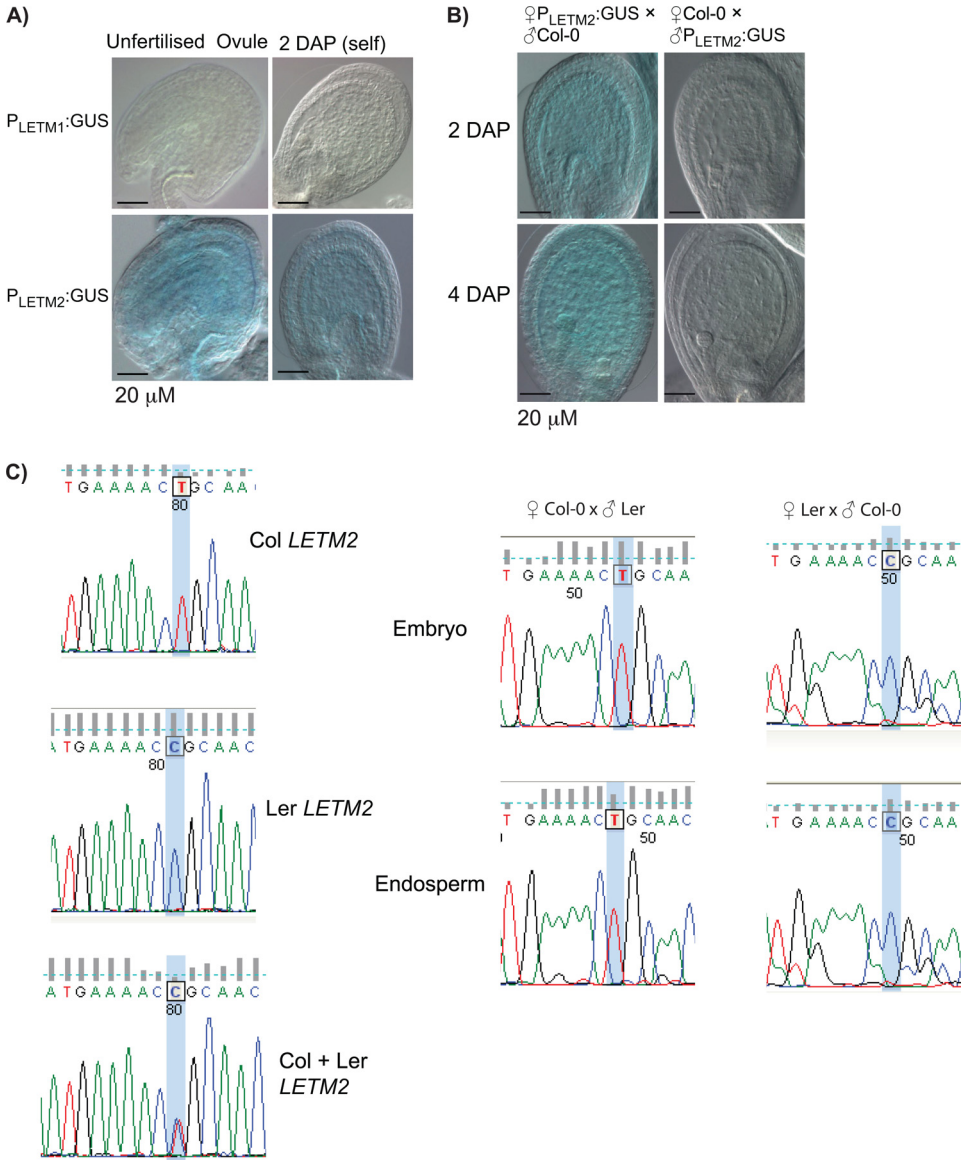

FIGURE 7. **LETM2 expression shows parent of origin effect.** *A*, expression pattern of AtLETM1::GUS and AtLETM2::GUS promoter reporter plants in unfertilized ovules and 2 days after self-pollination (*DAP*). *B*, reciprocal crosses between *LETM2*::*GUS* and wild-type (Col-0) plants 2 and 4 days postpollination, respectively. No GUS activity is detected when of paternal origin. *C*, Sanger sequencing chromatograms of partial *LETM2* cDNA showing a polymorphism between Col-0 and L*er* ecotypes. *Col-0* + *Ler*, artificial 1:1 mix of Col-0 and L*er* cDNA as control for equal sequencing efficiency of the polymorphism. Reciprocal crosses of Col-0 with L*er* indicate that the maternal cDNA is predominant. *Scale bars*, 50 μm.

that the stability or insertion of organelle-encoded subunits of the ATP synthase is affected. The detection of a protein complex in BN-PAGE with several subunits of ATP synthase with HSP60 is consistent with this (Fig. 4*B*). Thus, it is possible that LETM proteins are required for the correct orientation of ribosomes for efficient co-translational insertion of subunit 9 into the membrane and that limiting the abundance of LETM proteins results in degradation of subunit 9 that is not correctly inserted into the inner membrane, akin to the role played by Mba1 in yeast in assembly of cytochrome oxidase (66). Although this possibility cannot be excluded, it is notable that the accumulation of soluble subunit ATPα is also reduced, but not the nucleus-encoded β-subunit of F_1, suggesting that the rate of synthesis is affected. The smaller differences in incorporation of [^{35}S]Met at 30 min may simply reflect that all of the amino acids required for *in organelle* translation need to be transported across the inner mitochondrial membrane, and thus the difference in capacity for translation may only become apparent after some time, when all added amino acids are not limiting in the mitochondrial matrix.

It was determined that maternal *LETM2* was absolutely required for seed development; otherwise, the seed aborted at an early stage. Three independent methods support the biased parent of origin effect for LETM2. (i) The ratio of viable and aborted embryos in reciprocal crosses is indicative of a parent of origin affect but does not rule out a gametophyte affect. However, analysis of unfertilized ovules and pollen revealed normal development prior to fertilization. (ii) Reciprocal crosses of *LETM2*::*GUS* promoter reporter lines with Col-0 clearly demonstrated that the paternal *LETM2* promoter was silenced during early embryogenesis, and the maternal *LETM2* promoter

was active in female gametophyte before pollination and during early seed development. (iii) By analyzing maternal and paternal transcripts by dissecting endosperm and embryo tissues, we found that *LETM2* transcripts are of maternal origin for both embryo and endosperm as late as 6 days after pollination. Furthermore, the silencing of the *LETM2* promoter GUS construct hints at the mechanism that may underlie the parent of origin effect observed. The presence of an LTR/Gypsy transposon (AT1TE80065) in the promoter region of *AtLETM2* may act as a target site for methylation and the silencing observed via RNA-directed DNA methylation (56). Analysis of pollen and female gametophyte viability indicated that although the amount of pollen produced is reduced, the viability of the gametes is not affected. Thus, the failure of embryo development is due to a lack of expression in the early stages of seed development. Finally, analysis of the spatial expression pattern of AtLETM1 using AtLETM1 promoter GUS plants revealed that it was not detected in early endosperm or embryo (Fig. 7*C*), revealing that *in planta*, under normal situations, only the maternal *AtLETM2* controls translation of mRNA of mitochondrially encoded genes.

Although a number of studies have defined a variety of genes that display a biased parent of origin effect during early seed development, these genes encode proteins that are located in the nucleus or involved with regulation of nuclear genes and hormonal signaling pathways (52). Because biased parent of origin expression is proposed to occur due to the parent conflict hypothesis (15), it is consistent that mitochondrial gene expression is also under maternal control during early development (48). Early embryo development following fertilization and the earliest events in germination are crucial for plant development and success. The production of multiple offspring with potentially many different parental inputs would select for vigor in early embryo development and germination in parental gametes because they could out-compete other siblings for resources. However the maternal parent can counteract any such parental vigor by ensuring equal resource allocation during embryo development and early seedling development, after which environmental resources dominate growth and development. Given the essential role of mitochondrial function in embryo development and early germination, maternal control of mitochondrial gene expression ensures equal allocation to all offspring. Furthermore, maternal control of translation of mitochondrial genes could act to coordinate organelle and nuclear genome expression at the earliest stages of development because several nuclear genes have been characterized to display a biased maternal expression pattern that affects nuclear gene expression. Finally, given that the AtLETM protein contains an EF-hand domain and that *AtLETM1* is stress-inducible, it is suggested that mitochondrial gene expression at the level of translation may play a role in stress responses.

REFERENCES

1. Dyall, S. D., Brown, M. T., and Johnson, P. J. (2004) Ancient invasions. From endosymbionts to organelles. *Science* **304,** 253–257
2. Burger, G., Gray, M. W., and Lang, B. F. (2003) Mitochondrial genomes. Anything goes. *Trends Genet.* **19,** 709–716
3. Gray, M. W., Burger, G., and Lang, B. F. (1999) Mitochondrial evolution. *Science* **283,** 1476–1481
4. Gray, M. W., Burger, G., and Lang, B. F. (2001) The origin and early evolution of mitochondria. *Genome Biol.* **2,** REVIEWS1018
5. Gray, M. W., Lang, B. F., and Burger, G. (2004) Mitochondria of protists. *Annu. Rev. Genet.* **38,** 477–524
6. Daley, D. O., and Whelan, J. (2005) Why genes persist in organelle genomes. *Genome Biol.* **6,** 110
7. Schmidt, O., Pfanner, N., and Meisinger, C. (2010) Mitochondrial protein import. From proteomics to functional mechanisms. *Nat. Rev. Mol. Cell Biol.* **11,** 655–667
8. Giraud, E., Van Aken, O., Uggalla, V., and Whelan, J. (2012) REDOX regulation of mitochondrial function in plants. *Plant Cell Environ.* **35,** 271–280
9. Fujii, S., and Small, I. (2011) The evolution of RNA editing and pentatricopeptide repeat genes. *New Phytol.* **191,** 37–47
10. Giegé, P., Sweetlove, L. J., Cognat, V., and Leaver, C. J. (2005) Coordination of nuclear and mitochondrial genome expression during mitochondrial biogenesis in *Arabidopsis*. *Plant Cell* **17,** 1497–1512
11. Birky, C. W., Jr. (1995) Uniparental inheritance of mitochondrial and chloroplast genes. Mechanisms and evolution. *Proc. Natl. Acad. Sci. U.S.A.* **92,** 11331–11338
12. Bentley, K. E., Mandel, J. R., and McCauley, D. E. (2010) Paternal leakage and heteroplasmy of mitochondrial genomes in *Silene vulgaris*. Evidence from experimental crosses. *Genetics* **185,** 961–968
13. Matsushima, R., Tang, L. Y., Zhang, L., Yamada, H., Twell, D., and Sakamoto, W. (2011) A conserved, Mg^{2+}-dependent exonuclease degrades organelle DNA during *Arabidopsis* pollen development. *Plant Cell* **23,** 1608–1624
14. Feil, R., and Berger, F. (2007) Convergent evolution of genomic imprinting in plants and mammals. *Trends Genet.* **23,** 192–199
15. Haig, D., and Westoby, M. (1989) Parent-specific gene expression and the triploid endosperm. *Am. Nat.* **134,** 147–155
16. Bauerschmitt, H., Mick, D. U., Deckers, M., Vollmer, C., Funes, S., Kehrein, K., Ott, M., Rehling, P., and Herrmann, J. M. (2010) Ribosome-binding proteins Mdm38 and Mba1 display overlapping functions for regulation of mitochondrial translation. *Mol. Biol. Cell* **21,** 1937–1944
17. Schlickum, S., Moghekar, A., Simpson, J. C., Steglich, C., O'Brien, R. J., Winterpacht, A., and Endele, S. U. (2004) *LETM1*, a gene deleted in Wolf-Hirschhorn syndrome, encodes an evolutionarily conserved mitochondrial protein. *Genomics* **83,** 254–261
18. Dimmer, K. S., Fritz, S., Fuchs, F., Messerschmitt, M., Weinbach, N., Neupert, W., and Westermann, B. (2002) Genetic basis of mitochondrial function and morphology in *Saccharomyces cerevisiae*. *Mol. Biol. Cell* **13,** 847–853
19. Nowikovsky, K., Froschauer, E. M., Zsurka, G., Samaj, J., Reipert, S., Kolisek, M., Wiesenberger, G., and Schweyen, R. J. (2004) The LETM1/YOL027 gene family encodes a factor of the mitochondrial K^+ homeostasis with a potential role in the Wolf-Hirschhorn syndrome. *J. Biol. Chem.* **279,** 30307–30315
20. Jiang, D., Zhao, L., and Clapham, D. E. (2009) Genome-wide RNAi screen identifies Letm1 as a mitochondrial Ca^{2+}/H^+ antiporter. *Science* **326,** 144–147
21. Herrmann, J. M., Woellhaf, M. W., and Bonnefoy, N. (2012) *Biochim. Biophys. Acta*, in press
22. Boyes, D. C., Zayed, A. M., Ascenzi, R., McCaskill, A. J., Hoffman, N. E., Davis, K. R., and Görlach, J. (2001) Growth stage-based phenotypic analysis of *Arabidopsis*. A model for high throughput functional genomics in plants. *Plant Cell* **13,** 1499–1510
23. Carrie, C., Murcha, M. W., Kuehn, K., Duncan, O., Barthet, M., Smith, P. M., Eubel, H., Meyer, E., Day, D. A., Millar, A. H., and Whelan, J. (2008) Type II NAD(P)H dehydrogenases are targeted to mitochondria and chloroplasts or peroxisomes in *Arabidopsis thaliana*. *FEBS Lett.* **582,** 3073–3079
24. Carrie, C., Kühn, K., Murcha, M. W., Duncan, O., Small, I. D., O'Toole, N., and Whelan, J. (2009) Approaches to defining dual-targeted proteins in *Arabidopsis*. *Plant J.* **57,** 1128–1139
25. Lister, R., Carrie, C., Duncan, O., Ho, L. H., Howell, K. A., Murcha, M. W.,

and Whelan, J. (2007) Functional definition of outer membrane proteins involved in preprotein import into mitochondria. *Plant Cell* **19,** 3739–3759
26. Kühn, K., Richter, U., Meyer, E. H., Delannoy, E., de Longevialle, A. F., O'Toole, N., Börner, T., Millar, A. H., Small, I. D., and Whelan, J. (2009) Phage-type RNA polymerase RPOTmp performs gene-specific transcription in mitochondria of *Arabidopsis thaliana*. *Plant Cell* **21,** 2762–2779
27. Whelan, J., Smith, M. K., Meijer, M., Yu, J. W., Badger, M. R., Price, G. D., and Day, D. A. (1995) Cloning of an additional cDNA for the alternative oxidase in tobacco. *Plant Physiol.* **107,** 1469–1470
28. Bathgate, B., Baker, A., and Leaver, C. J. (1989) Two genes encode the adenine nucleotide translocator of maize mitochondria. Isolation, characterisation, and expression of the structural genes. *Eur. J. Biochem.* **183,** 303–310
29. Murcha, M. W., Elhafez, D., Millar, A. H., and Whelan, J. (2004) The N-terminal extension of plant mitochondrial carrier proteins is removed by two-step processing. The first cleavage is by the mitochondrial processing peptidase. *J. Mol. Biol.* **344,** 443–454
30. Cooper, H. M., and Paterson, Y. (2009) Production of polyclonal antisera. *Curr. Protoc. Neurosci.* Chapter 5, Unit 5.5
31. Carrie, C., Giraud, E., Duncan, O., Xu, L., Wang, Y., Huang, S., Clifton, R., Murcha, M., Filipovska, A., Rackham, O., Vrielink, A., and Whelan, J. (2010) Conserved and novel functions for *Arabidopsis thaliana* MIA40 in assembly of proteins in mitochondria and peroxisomes. *J. Biol. Chem.* **285,** 36138–36148
32. Lamattina, L., Gonzalez, D., Gualberto, J., and Grienenberger, J. M. (1993) Higher plant mitochondria encode an homologue of the nuclear-encoded 30-kDa subunit of bovine mitochondrial complex I. *Eur. J. Biochem.* **217,** 831–838
33. Considine, M. J., Daley, D. O., and Whelan, J. (2001) The expression of alternative oxidase and uncoupling protein during fruit ripening in mango. *Plant Physiol.* **126,** 1619–1629
34. Murcha, M. W., Elhafez, D., Millar, A. H., and Whelan, J. (2005) The C-terminal region of TIM17 links the outer and inner mitochondrial membranes in *Arabidopsis* and is essential for protein import. *J. Biol. Chem.* **280,** 16476–16483
35. Karimi, M., Inzé, D., and Depicker, A. (2002) GATEWAY vectors for *Agrobacterium*-mediated plant transformation. *Trends Plant Sci.* **7,** 193–195
36. Giraud, E., Van Aken, O., Ho, L. H., and Whelan, J. (2009) The transcription factor ABI4 is a regulator of mitochondrial retrograde expression of ALTERNATIVE OXIDASE1a. *Plant Physiol.* **150,** 1286–1296
37. Luo, M., Dennis, E. S., Berger, F., Peacock, W. J., and Chaudhury, A. (2005) MINISEED3 (MINI3), a WRKY family gene, and HAIKU2 (IKU2), a leucine-rich repeat (LRR) KINASE gene, are regulators of seed size in *Arabidopsis*. *Proc. Natl. Acad. Sci. U.S.A.* **102,** 17531–17536
38. Alexander, M. P. (1969) Differential staining of aborted and nonaborted pollen. *Stain Technol.* **44,** 117–122
39. Kühn, K., Carrie, C., Giraud, E., Wang, Y., Meyer, E. H., Narsai, R., des Francs-Small, C. C., Zhang, B., Murcha, M. W., and Whelan, J. (2011) The RCC1 family protein RUG3 is required for splicing of nad2 and complex I biogenesis in mitochondria of *Arabidopsis thaliana*. *Plant J.* **67,** 1067–1080
40. Baldi, P., and Long, A. D. (2001) A Bayesian framework for the analysis of microarray expression data. Regularized *t*-test and statistical inferences of gene changes. *Bioinformatics* **17,** 509–519
41. Benjamini, Y., and Hochberg, Y. (1995) Controlling the false discovery rate. A practical and powerful approach to multiple testing. *J. R. Stat. Soc. Ser. B* **57,** 289–300
42. Gleason, C., Huang, S., Thatcher, L. F., Foley, R. C., Anderson, C. R., Carroll, A. J., Millar, A. H., and Singh, K. B. (2011) Mitochondrial complex II has a key role in mitochondrial-derived reactive oxygen species influence on plant stress gene regulation and defense. *Proc. Natl. Acad. Sci. U.S.A.* **108,** 10768–10773
43. Eubel, H., Braun, H. P., and Millar, A. H. (2005) Blue-native PAGE in plants. A tool in analysis of protein-protein interactions. *Plant Methods* **1,** 11
44. Meyer, E. H., Heazlewood, J. L., and Millar, A. H. (2007) Mitochondrial acyl carrier proteins in *Arabidopsis thaliana* are predominantly soluble matrix proteins and none can be confirmed as subunits of respiratory Complex I. *Plant Mol. Biol.* **64,** 319–327
45. Van Aken, O., Zhang, B., Carrie, C., Uggalla, V., Paynter, E., Giraud, E., and Whelan, J. (2009) Defining the mitochondrial stress response in *Arabidopsis thaliana*. *Mol. Plant* **2,** 1310–1324
46. Endele, S., Fuhry, M., Pak, S. J., Zabel, B. U., and Winterpacht, A. (1999) LETM1, a novel gene encoding a putative EF-hand Ca^{2+}-binding protein, flanks the Wolf-Hirschhorn syndrome (WHS) critical region and is deleted in most WHS patients. *Genomics* **60,** 218–225
47. Frazier, A. E., Taylor, R. D., Mick, D. U., Warscheid, B., Stoepel, N., Meyer, H. E., Ryan, M. T., Guiard, B., and Rehling, P. (2006) Mdm38 interacts with ribosomes and is a component of the mitochondrial protein export machinery. *J. Cell Biol.* **172,** 553–564
48. Law, S. R., Narsai, R., Taylor, N. L., Delannoy, E., Carrie, C., Giraud, E., Millar, A. H., Small, I., and Whelan, J. (2012) Nucleotide and RNA metabolism prime translational initiation in the earliest events of mitochondrial biogenesis during *Arabidopsis* germination. *Plant Physiol.* **158,** 1610–1627
49. Millar, A. H., Whelan, J., Soole, K. L., and Day, D. A. (2011) Organization and regulation of mitochondrial respiration in plants. *Annu. Rev. Plant. Biol.* **62,** 79–104
50. Dutilleul, C., Garmier, M., Noctor, G., Mathieu, C., Chétrit, P., Foyer, C. H., and de Paepe, R. (2003) Leaf mitochondria modulate whole cell redox homeostasis, set antioxidant capacity, and determine stress resistance through altered signaling and diurnal regulation. *Plant Cell* **15,** 1212–1226
51. Karpova, O. V., Kuzmin, E. V., Elthon, T. E., and Newton, K. J. (2002) Differential expression of alternative oxidase genes in maize mitochondrial mutants. *Plant Cell* **14,** 3271–3284
52. Ikeda, Y. (2012) Plant imprinted genes identified by genome-wide approaches and their regulatory mechanisms. *Plant Cell Physiol.* **53,** 809–816
53. Unseld, M., Marienfeld, J. R., Brandt, P., and Brennicke, A. (1997) The mitochondrial genome of *Arabidopsis thaliana* contains 57 genes in 366,924 nucleotides. *Nat. Genet.* **15,** 57–61
54. Heazlewood, J. L., Whelan, J., and Millar, A. H. (2003) The products of the mitochondrial *orf25* and *orfB* genes are FO components in the plant F1FO ATP synthase. *FEBS Lett.* **540,** 201–205
55. Chacinska, A., Koehler, C. M., Milenkovic, D., Lithgow, T., and Pfanner, N. (2009) Importing mitochondrial proteins. Machineries and mechanisms. *Cell* **138,** 628–644
56. Haag, J. R., and Pikaard, C. S. (2011) Multisubunit RNA polymerases IV and V. Purveyors of non-coding RNA for plant gene silencing. *Nat. Rev. Mol. Cell Biol.* **12,** 483–492
57. Christensen, C. E., King, E. J., Jordan, J. R., and Drews, G. N. (1997) Megagametogenesis in *Arabidopsis* wild type and the Gf mutant. *Sex. Plant Reprod.* **10,** 49–67
58. Webb, M. C., and Gunning, B. E. S. (1990) Embryo sac development in *Arabidopsis thaliana*. I. Megasporogenesis including the microtubular cytoskeleton. *Sex. Plant Reprod.* **3,** 244–256
59. Webb, M. C., and Gunning, B. E. S. (1994) Embryo sac development in *Arabidopsis thaliana* II. The cytoskeleton during megagametogenesis. *Sex. Plant Reprod.* **7,** 153–163
60. Boisnard-Lorig, C., Colon-Carmona, A., Bauch, M., Hodge, S., Doerner, P., Bancharel, E., Dumas, C., Haseloff, J., and Berger, F. (2001) Dynamic analyses of the expression of the HISTONE::YFP fusion protein in *Arabidopsis* show that syncytial endosperm is divided in mitotic domains. *Plant Cell* **13,** 495–509
61. Grini, P. E., Jürgens, G., and Hülskamp, M. (2002) Embryo and endosperm development is disrupted in the female gametophytic capulet mutants of *Arabidopsis*. *Genetics* **162,** 1911–1925
62. Klodmann, J., Senkler, M., Rode, C., and Braun, H. P. (2011) Defining the protein complex proteome of plant mitochondria. *Plant Physiol.* **157,** 587–598
63. Rode, C., Senkler, M., Klodmann, J., Winkelmann, T., and Braun, H. P.

(2011) GelMap. A novel software tool for building and presenting proteome reference maps. *J. Proteomics* **74,** 2214–2219
64. Rak, M., Zeng, X., Brière, J. J., and Tzagoloff, A. (2009) Assembly of F_0 in *Saccharomyces cerevisiae*. *Biochim. Biophys. Acta* **1793,** 108–116
65. Geisler, D. A., Päpke, C., Obata, T., Nunes-Nesi, A., Matthes, A., Schneitz, K., Maximova, E., Araújo, W. L., Fernie, A. R., and Persson, S. (2012) Down-regulation of the δ-subunit reduces mitochondrial ATP synthase levels, alters respiration, and restricts growth and gametophyte development in *Arabidopsis*. *Plant Cell* **24,** 2792–2811
66. Ott, M., and Herrmann, J. M. (2010) Co-translational membrane insertion of mitochondrially encoded proteins. *Biochim. Biophys. Acta* **1803,** 767–775